

Learning Personalized Decision Support Policies

Umang Bhatt^{*1,2}, Valerie Chen^{*3}, Katherine M. Collins¹, Parameswaran Kamalaruban²,
Emma Kallina¹, Adrian Weller^{1,2}, and Ameet Talwalkar³

¹University of Cambridge

²The Alan Turing Institute

³Carnegie Mellon University

Abstract

Individual human decision-makers may benefit from different forms of support to improve decision outcomes. However, a key question is *which* form of support will lead to accurate decisions at a low cost. In this work, we propose learning a *decision support policy* that, for a given input, chooses which form of support, if any, to provide. We consider decision-makers for whom we have no prior information and formalize learning their respective policies as a multi-objective optimization problem that trades off accuracy and cost. Using techniques from stochastic contextual bandits, we propose **THREAD**, an online algorithm to personalize a decision support policy for each decision-maker, and devise a hyper-parameter tuning strategy to identify a cost-performance trade-off using simulated human behavior. We provide computational experiments to demonstrate the benefits of **THREAD** compared to offline baselines. We then introduce **Modiste**, an interactive tool that provides **THREAD** with an interface. We conduct human subject experiments to show how **Modiste** learns policies personalized to each decision-maker and discuss the nuances of learning decision support policies online for real users.

1 Introduction

To improve outcomes, human decision-makers can use various forms of support to alter their opinions before making a final decision [1]. For a given input, different decision-makers may benefit from different forms of support. For example, one radiologist may provide a better diagnosis of a chest X-ray by leveraging model predictions [2] while another may perform better after viewing suggestions from senior radiologists [3] or viewing a summary of relevant medical records from a large language model (LLM) [4, 5, 6, 7]. An individual decision-maker may also need a different form of support for different inputs. In this paper, we study how to improve decision-making performance by *personalizing* which form of support we provide to a decision-maker on a case-by-case basis, as illustrated in Figure 1.

We formalize learning a *decision support policy* that dictates what type of additional support, if any, should be presented for a given input as a multi-objective optimization problem. One of our objectives is to provide support that improves a specific decision-maker’s performance. Since providing support may be costly [8, 9], a second objective is to minimize the cost of the selected support. More specifically, our goal is to identify a personalized decision support policy for a given decision-maker that minimizes the incurred cost of support while ensuring that the decision-maker’s accuracy meets a specified threshold.

To learn decision support policies, prior works assume access to offline human decisions under support [10, 11] or oracle queries of human behavior [12, 13]. We argue that it is unrealistic in

^{*}Both authors contributed equally. Order was decided by a coin flip. Correspondence to: valeriechen@cmu.edu and usb20@cam.ac.uk

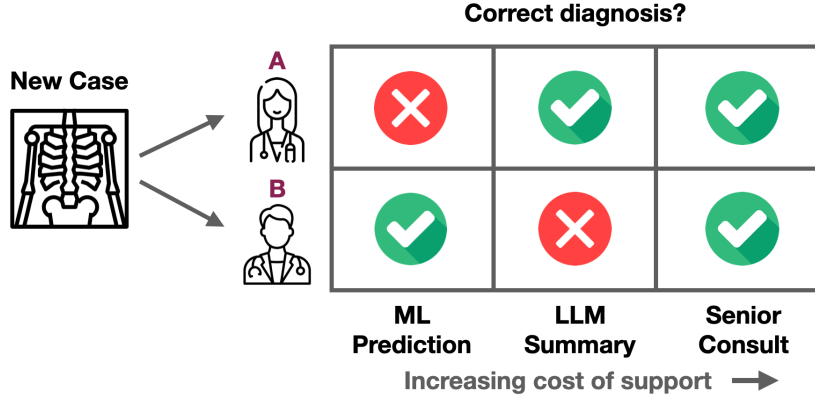


Figure 1: We illustrate the importance of personalized decision support to balance decision-maker correctness and the cost of support. While both decision-makers are correct after a costly senior consult for this input, decision-maker A’s policy should suggest providing an ML prediction but decision-maker B’s policy should recommend an LLM summary. In this work, we propose an online formulation to learn decision support policies without assuming access to any offline data about a given decision-maker.

practice to assume an offline dataset of decisions *for a new decision-maker* with all available forms of support can be obtained. Thus, for individuals for whom we have no prior information, we propose learning how to personalize support in an *online* setting.

We introduce **THREAD**, an algorithm for learning decision support policies online given a parameter that governs the trade-off between performance and cost. At its core, **THREAD** sequentially estimates the prediction error of a decision-maker under each form of support by applying techniques from the stochastic contextual bandit literature [14]. Since it is common to specify a performance threshold in practice, we develop a novel hyper-parameter tuning strategy to identify a trade-off parameter that corresponds to a given performance threshold. This strategy uses simulated human decision-makers to explore different choices of the trade-off parameter and selects one to use for **THREAD** in deployment on real-world decision-makers.

We conduct computational experiments to explore whether **THREAD** achieves a prescribed performance threshold across a variety of simulated decision-makers. We demonstrate that policies learned using **THREAD** outperform baselines, including fixed policies that always provide a particular form of support and offline population-level decision support policies. We find that offline population policies struggle to adequately support new decision-makers, affirming the need to personalize decision support policies online.

We conduct human subject experiments where we use **THREAD** to learn decision support policies online, whereas prior work only tests offline policies or evaluates in simulation. To test our methods in practice, we develop **Modiste**,¹ an interactive tool that gives **THREAD** an interface. We demonstrate that **Modiste** can be used to learn personalized decision support policies on both vision and language tasks, where we explore forms of support that include expert consensus or predictions from an LLM. We also discuss the challenges of deploying decision support policies in practice (e.g., issues of decision-maker adherence to the support provided and the potential gap between human simulators and real participants). These findings strongly suggest the importance of running human subject experiments to validate any proposed decision support algorithm.

In summary, our contributions are as follows:

- We propose a multi-objective optimization formulation of learning a decision support policy that trades off performance and cost. We introduce **THREAD**, an online algorithm to learn such a policy, and devise a hyper-parameter tuning strategy, which finds a trade-off parameter that minimizes cost and achieves a specified performance threshold.

¹While a “modiste” usually refers to someone who tailors clothing and makes dresses/hats, we use the term to capture our tool’s ability to alter a policy to a decision-maker.

- We demonstrate the importance of online learning to personalize policies to new decision-makers through both computational and human subject experiments. We develop an interactive tool, **Modiste**, to incorporate **THREAD** into an interface. We use **Modiste** to conduct human subject experiments that evaluate the efficacy of our formulation with real users on vision and language tasks.

2 Related Work

Overview of Decision Support. There are various forms of decision support proposed in the literature, such as expert consensus [15] and changes to machine interfaces [16]. More recent forms of decision support include algorithmic tools where decision-makers are aided by predictive systems. There is a particular focus on support from ML models [17]. While the primary objective of providing support is to increase decision-maker *performance*, the *cost* of providing such support has also been studied [18]. In this work, we account for both performance and cost as a multi-objective optimization problem (e.g., there is usually a trade-off between the cost of support and how much decision outcomes improve given a form of support).

Comparison to Prior Decision Support Set-ups. In many prior works, the human does not always make the final decision. For example, in the learning to defer paradigm [19, 13], the system routes between model and human decisions. Similarly, others have jointly learned an allocation function between a model and a pool of decision makers [20, 21]. In our setting, the *human* is always the decision-maker, which reflects many real-world applications. The specific set-up, where humans make the final decisions with support from ML models, has been referred to as “algorithm-in-the-loop” [22] and has been studied in many HCI studies [23]. Prior set-ups have also studied how humans make decisions when provided with additional information on top of the ML model prediction (e.g., explanations [24], uncertainty [25], conformal sets [26]). However, these studies *always* show one particular form of support. Our work can not only consider the forms of support in these studies but also formalizes *learning* in what contexts each form of support should be provided. An extensive comparison to prior work is in Appendix A.

Prior Assumptions About Decision-Maker Information. We briefly survey the assumptions made in prior work about the decision-maker when learning decision support policies. The model of the decision maker is either synthetic, thus lacking grounding in actual human behavioral data, or learned from a batch of *offline* annotations [19, 27, 11, 28]. For a new decision-maker or a new form of support, this set of data would not be available in practice. Instead, we propose to learn a decision support policy *online* to circumvent these limitations. There are few works that use some aspect of online learning for different decision-making settings or under strict theoretical conditions, as we describe in Appendix A.

Background on Online Learning. Learning decision support policies can be done with bandit feedback, where at each time step the learner receives a reward based on a selected action. The problem is a case of stochastic contextual bandits [14], where the reward depends on the context which are sampled i.i.d. In our setting, the contexts are the input, the actions represent the forms of support, and the reward depends on a decision-maker’s decision, which in turn provides bandit feedback online. We propose a framework to learn decision support policies that can use existing techniques from the contextual bandits literature, LinUCB [14] and KNN-UCB [29]. While we formulate learning decisions support policies as a multi-objective problem, prior work on multi-objective contextual bandits [30, 31] makes theoretical assumptions that are not applicable in our setting. Instead, we reduce the multi-objective to a single-objective problem and propose a practical hyper-tuning strategy for that parameter.

3 Problem Formulation

In this section, we provide a formal description of a human decision-making process under various forms of decision support. We propose a multi-objective optimization problem to capture trade-offs between the cost of support and the decision outcome for a given form of support. We then cast the multi-objective problem into a single-objective and discuss how to evaluate the resultant decision support policy subject to a desired performance threshold.

3.1 Problem Setting

We consider a human decision-making process with different forms of decision support. In particular, we focus on a multi-class classification problem with observation/feature space $\mathcal{X} \subseteq \mathbb{R}^p$ and outcome/label space $\mathcal{Y} = [K]$. We concentrate on a stochastic setting where the data $(x, y) \in \mathcal{X} \times \mathcal{Y}$ are drawn iid from a fixed, unknown data generating distribution \mathcal{P} , an assumption that reflects typical decision-making settings. In addition, we consider an action set \mathcal{A} corresponding to the forms of support available. Given an observation $x \in \mathcal{X}$, the human attempts to predict the corresponding label $y \in \mathcal{Y}$ using the support prescribed by an action $a \in \mathcal{A}$, i.e., the human makes the prediction using an unknown function $h : \mathcal{X} \times \mathcal{A} \rightarrow \mathcal{Y}$. *Our problem formulation and algorithms to solve the formulation are agnostic to the specific forms of support*; we provide multiple instantiations in later human subject experiments. The cost of using different support is given by $c : \mathcal{A} \rightarrow [0, 1]$. The quality of the final prediction made by the human is measured by a loss function $\ell : \mathcal{Y} \times \mathcal{Y} \rightarrow [0, 1]$ w.r.t. the true label. We consider a 0-1 loss function, where $\ell(y, y') = 1$ for $y \neq y'$ and $\ell(y, y') = 0$ for $y = y'$.

Decision-Making Protocol. We aim to learn a policy $\pi : \mathcal{X} \rightarrow \Delta(\mathcal{A})$ that picks the appropriate form of support to assist a new decision-maker. Let Π denote the class of all stochastic decision support policies. Let $\mathcal{A} = \{A_1, \dots, A_k\}$, and $\pi(x)_{A_i}$ denote $\mathbb{P}[A_i \sim \pi(x)]$ for each $A_i \in \mathcal{A}$. When $A_i \sim \pi(x)$, the human decision-maker makes the prediction \tilde{y} based on the observation x and support prescribed by A_i , i.e., the final prediction \tilde{y} is given by $\tilde{y} = h(x, A_i)$. The human decision-making process with different forms of support is described below. For $t = 1, 2, \dots, T$:

1. A data point $(x_t, y_t) \in \mathcal{X} \times \mathcal{Y}$ is drawn iid from \mathcal{P} .
2. A form of support $a_t \in \mathcal{A}$ is selected using a decision support policy $\pi_t : \mathcal{X} \rightarrow \Delta(\mathcal{A})$.
3. The human decision-maker makes the final prediction $\tilde{y}_t = h(x_t, a_t)$ based on x_t and a_t .
4. The human decision-maker incurs a loss $\ell(y_t, \tilde{y}_t) = 1$ if $y_t \neq \tilde{y}_t$ and $\ell(y_t, \tilde{y}_t) = 0$ otherwise.

A static decision support policy, where the policy does not change throughout the interaction with the decision-maker, could be deployed. This approach reflects many prior user studies, per Lai et al. [23]; for example, decision-makers may *always* be presented with the predictions of an ML model. Additionally, it is possible to update a policy π_t iteratively at each time step based on the most recent interaction with the decision-maker, i.e., using $\{(x_t, y_t, a_t, \tilde{y}_t)\}$. We propose a method to make such an update online in Section 4.

3.2 Learning Objectives

At each time step t , we evaluate the current policy π_t based on two objectives: (i) the loss of the decision-maker’s prediction under the form of support selected by the policy π_t , and (ii) the cost associated with that form of support. We formalize these objectives below.

For any policy π , the expected loss incurred by the decision-maker under policy π is given by:

$$r_h(\pi) = \mathbb{E}_{(x,y) \sim \mathcal{P}} [\mathbb{E}_{A_i \sim \pi(x)} [\ell(y, h(x, A_i))]] = \mathbb{E}_x \left[\sum_{i=1}^k \pi(x)_{A_i} \cdot \mathbb{E}_{y|x} [\ell(y, h(x, A_i))] \right]. \quad (1)$$

Further, the expected cost of the policy π is given by:

$$c(\pi) = \mathbb{E}_x \left[\sum_{i=1}^k \pi(x)_{A_i} \cdot c(A_i) \right]. \quad (2)$$

Given these two objectives, we consider the following multi-objective optimization (MOO):

$$\min_{\pi} \mathcal{R}_h(\pi) = [r_h(\pi), c(\pi)]^\top. \quad (3)$$

In subsequent evaluations, irrespective of the method used to learn a decision support policy, we evaluate the quality of a policy at a given time π_t by considering its expected loss $r_h(\pi_t)$, and expected cost $c(\pi_t)$. We use expected performance to measure generalization across inputs, rather than instantaneous performance on a single data point (x_t, y_t) .

3.3 Reframing the Objective

We first reformulate this MOO problem into a single-objective optimization (SOO) problem:

$$\pi_\lambda^* = \arg \min_{\pi \in \Pi} \lambda \cdot r_h(\pi) + (1 - \lambda) \cdot c(\pi), \quad (4)$$

where $\lambda \in [0, 1]$. It can be shown that the solutions of the SOO problem can fully characterize the Pareto front of the MOO problem, i.e., any Pareto optimal policy of the MOO problem is a solution to the SOO problem for some choice of $\lambda \in [0, 1]$ [32, 33]. The formal statements are provided in Appendix B.1. For any given $\lambda \in [0, 1]$, our goal is to develop an online learning algorithm to find the solution π_λ^* to the SOO problem in Eq. 4. We observe that we can rewrite the SOO problem as follows (see Appendix B.2):

$$\pi_\lambda^*(x) = \arg \min_{A_i \in \mathcal{A}} \lambda \cdot r_{A_i}(x; h) + (1 - \lambda) \cdot c(A_i), \quad (5)$$

where $r_{A_i}(x; h) = \mathbb{E}_{y|x}[\ell(y, h(x, A_i))]$ is the human prediction error for input x and support A_i . This simplified form of π_λ^* enables us to propose an efficient strategy to learn the policy online by estimating $r_{A_i}(x; h)$ value via interaction with the decision-maker h . It is nontrivial to identify the appropriate modeling assumptions for h under all forms of support [34]; thus, for the purposes of learning which form of support to provide, we focus on learning $r_{A_i}(x; h)$ for a given h .

3.4 Evaluating Policies in Practice

In practice, we want to learn a policy that achieves a certain level of performance at a minimal cost. That is, given a tolerance threshold $\epsilon \in [0, 1]$ for the expected loss, our goal is to learn a decision support policy π that achieves minimum expected cost while maintaining the expected loss that is within ϵ of the optimal loss r_h^{opt} :

$$\pi^\epsilon = \arg \min_{\pi \in \Pi} c(\pi) \quad \text{such that} \quad r_h(\pi) \leq r_h^{\text{opt}} + \epsilon, \quad (6)$$

where $r_h^{\text{opt}} = \min_{\pi} r_h(\pi)$. However, it is unclear what the corresponding choice of λ is, if any, for a given ϵ and h . We observe that there exists a $\lambda(\epsilon) \in [0, 1]$ such that $\pi_{\lambda(\epsilon)}^* = \pi^\epsilon$ where $\pi^\epsilon \in \Pi_{\text{opt}} = \{\pi_\lambda^* : \lambda \in [0, 1]\}$ and Π_h^{opt} is the complete set of Pareto optimal policies for a given human h . Thus, we propose a hyper-parameter tuning strategy to find a λ that leads to a policy with an expected loss of no more than ϵ above r_h^{opt} .

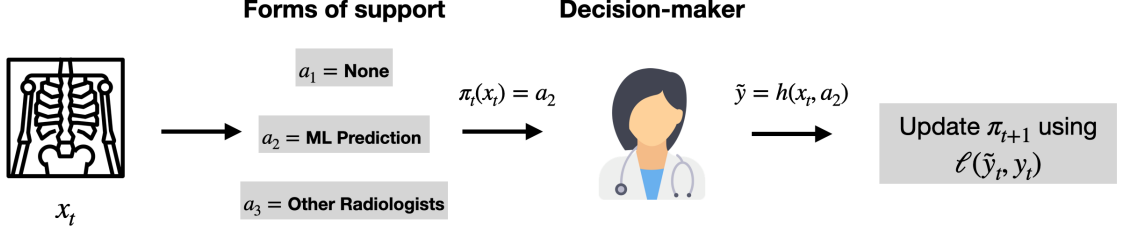


Figure 2: We illustrate the process of learning a decision support policy π_t online to improve a decision-maker’s performance at a minimal added cost. For every decision, our policy selects a form of support $\pi_t(x_t)$ from a set \mathcal{A} (e.g., $a_1 = \text{No support}$, $a_2 = \text{Displaying predictions}$, $a_3 = \text{Consulting experts}$) to present for an input x_t . The policy is updated using $\ell(\tilde{y}_t, y_t)$, the loss incurred after observing a decision \tilde{y}_t . Our online formulation (1) provides policies for new decision-makers for whom no offline data has been collected and (2) personalizes a decision support policy to individual needs.

4 Methods

When faced with a new decision-maker, a lack of prior information can make it challenging to learn a personalized decision support policy. Obtaining an extensive offline dataset of human decision-making for an unseen decision-maker *with every form of support* may be difficult in practice. While we may have access to data from other decision-makers in the population, relying solely on population-level data may not suffice for a new decision-maker, who may have individual differences in how they make decisions or rely on support. In contrast to the discussion in Section 2, we propose a framework (Figure 2) for learning decision support policies *online*.²

First, in Section 4.1, we present an online learning algorithm, **THREAD**, to learn a decision support policy π_λ^* for any given $\lambda \in [0, 1]$ using Eq 5. To identify a parameter to deploy for a new decision-maker, we discuss a hyper-parameter tuning strategy that uses population-level data from either interaction data of other decision-makers or estimates of their $r_{A_i}(x; h)$ in Section 4.2. Exploring sample-efficient strategies that jointly identify suitable $\lambda(\epsilon)$ and the corresponding policy π^ϵ is worthy of further investigation.

4.1 THREAD

The human decision-making process with different forms of support, described in Section 3.1, can be modeled as a contextual bandit problem, where the forms of support are the arms and \mathcal{X} is the context space. Based on this insight, we present **THREAD**, outlined in Algorithm 1. **THREAD** is an algorithm for learning the policy π_λ^* online to solve Eq 5 for a given $\lambda \in [0, 1]$. We propose Steps 1 and 2 of the algorithm in a general way to work with any online learning method.

Policy Update Step 1. In Eq. 5, the costs of each support are given and fixed. The main unknown is the decision-maker’s prediction error under different forms of support. We discuss two approaches to estimate the human prediction error $r_{A_i}(x; h)$ for all $x \in \mathcal{X}$ and $A_i \in \mathcal{A}$.

First, we use LinUCB [14] to approximate expected loss $r_{A_i}(x; h)$ by a linear function, i.e., $r_{A_i}(x; h) \approx \hat{r}_{A_i}(x; h) := \langle \theta_{A_i}, x \rangle$. We learn the parameters $\{\theta_{A_i} : A_i \in \mathcal{A}\}$ using LinUCB with the instantaneous reward function $R(x, y, A_i; h) := \ell(y, h(x, A_i))$. We then normalize the values of $\hat{r}_{A_i}(x; h)$ to lie in the range $[0, 1]$.

Second, we use an intuitive K -nearest neighbor (KNN) approach, which is a simplified variant of KNN-UCB [29], to approximate the error values $r_{A_i}(x; h)$. Specifically, we maintain an evolving data buffer \mathcal{D}_t , where we accumulate the history of interactions with the decision-maker. For

²If we had additional information via offline datasets or prior knowledge on the new human decision-maker, we can likely incorporate that information into selecting $\lambda(\epsilon)$ or obtaining more accurate estimates of $\hat{r}_{A_i}(x; h)$ efficiently; however, considering such additional information is out of scope for this work.

Algorithm 1 THREAD

- 1: **Input:** trade-off parameter λ ; human decision-maker h ; cost function $c : \mathcal{A} \rightarrow [0, 1]$
- 2: **Initialization:** data buffer $\mathcal{D}_0 = \{\}$; human prediction error values $\{\hat{r}_{A_i,0}(x; h) = 0.5 : x \in \mathcal{X}, A_i \in \mathcal{A}\}$; initial policy π_1
- 3: **for** $t = 1, 2, \dots, T$ **do**
- 4: data point $(x_t, y_t) \in \mathcal{X} \times \mathcal{Y}$ is drawn iid from \mathcal{P}
- 5: support $a_t \in \mathcal{A}$ is selected using policy π_t
- 6: human makes the prediction \tilde{y}_t based on x_t and a_t
- 7: human incurs the loss $\ell(y_t, \tilde{y}_t)$
- 8: update the buffer $\mathcal{D}_t \leftarrow \mathcal{D}_{t-1} \cup \{(x_t, a_t, \ell(y_t, \tilde{y}_t))\}$
- 9: update the decision support policy:

$$\hat{r}_{A_i,t}(x; h) \leftarrow \mathcal{U}_r(\hat{r}_{A_i,t-1}(x; h), \mathcal{D}_t) \quad (\text{Step 1})$$

$$\pi_{t+1}(x) \leftarrow \mathcal{U}_\pi(\hat{r}_{A_i,t}, c, \lambda) \quad (\text{Step 2})$$

10: **end for**

11: **Output:** policy $\pi_\lambda^{\text{alg}} \leftarrow \pi_{T+1}$

any new observation x , we can estimate $\hat{r}_{A_i}(x; h)$ values by finding its K -nearest neighbors in \mathcal{D}_t and computing the average error of these neighbors.

Policy Update Step 2. As mentioned above, it is crucial to have accurate estimates of the human prediction error values (see Eq 5). To achieve this, one could use a pure exploratory policy π_{t+1} in Step 2 of Algorithm 1, where $\pi_{t+1}(x)_{A_i} = 1/|\mathcal{A}|$ for all $A_i \in \mathcal{A}$. However, this approach would require a large number of interactions T to achieve accurate error estimates. In practical settings, where interactions are limited, as in our human subject experiments, T tends to be relatively small, making this approach less feasible.

When trying to learn the policy π_λ^* for a given λ , one can improve sample efficiency by guiding exploration with the policy $\pi_{t+1}(x) = \arg \min_{A_i \in \mathcal{A}} \lambda \cdot \hat{r}_{A_i,t}(x; h) + (1 - \lambda) \cdot c(A_i)$ in Step 2 of Algorithm 1. Additionally, depending on the specific implementation, additional exploration terms can be used for better performance. In Appendix B.5, we present specific implementations of Algorithm 1 using LinUCB and online KNN.

4.2 Hyper-parameter selection for THREAD

While we introduce multiple algorithm-specific parameters in Section 4.1 (e.g., α for LinUCB and K , W , and γ for KNN), the hyper-parameter of primary interest is $\lambda(\epsilon)$.³ When learning a decision support policy online for a new decision-maker h , we need to identify a suitable λ that achieves an expected loss within ϵ of r_h^{opt} . However, it is difficult to test multiple λ values simultaneously for the new decision-maker without potentially repeating queries of the same input: we only have a finite number of interactions with the decision-maker before issues of cognitive load arise per Section 7. We now describe a strategy to select λ using population-level data. While the decision-makers in the population may differ from the unseen decision-maker, we prefer this principled starting point to a random selection of λ .

Constructing human simulators. For each of the m decision-makers in our population-level data, we construct a simulator by calculating $r_{A_i}(x; h_j)$ for all A_i , $x \in \mathcal{X}$, and $j \in [m]$. Each $r_{A_i}(x; h_j)$ is *agnostic* to the instantiation of the form of support and does not explicitly model how the decision-maker j leverages A_i . To capture human competencies across \mathcal{X} , we assume

³From here on, we drop the explicit dependence on ϵ for more concise notation.

that the input space is divided into regions where $r_{A_i}(x; h)$ is roughly the same across that region for a given form of support A_i . These regions may be defined by class labels or by covariates of the task. For example, we write $r_{A_1} = [0.7, 0.1, 0.7]$ to denote that, under observing support A_1 , the decision-maker incurs a risk of 0.7 on one region, of 0.1 on a second, and 0.7 on the third. We let $\{h_{\text{sim-1}}, \dots, h_{\text{sim-}m}\}$ denote the set of simulated decision-makers.

Selecting a trade-off parameter for deployment. We want to select a trade-off parameter to deploy THREAD with for an unseen human h_{real} . As a result, we apply THREAD (with the same cost structure $c(A_i)$ as that of the real decision-maker) on each simulated decision-maker $h_{\text{sim-}j}$ across a range of λ values to obtain a set of candidate policies. In our experiments, we evaluate a range of $\lambda \in [0, 1]$ values in increments of 0.05. From this set of candidate policies and their respective λ values, we decide which λ to deploy on h_{real} . We consider three selection strategies:

- A. **Most likely λ .** For each simulator, we identify the set of $\{\lambda_{\text{sim-}j}\}$, which yield policies that meet $r_{h_{\text{sim-}j}}^{\text{opt}} + \epsilon$. We then take the λ that occurs the *most often* across simulators. If no policy meets the threshold for $h_{\text{sim-}j}$, we select the policy closest to $r_{h_{\text{sim-}j}}^{\text{opt}}$, which can be computed given r_{A_i} for all x for each simulated decision-maker.
- B. **Most likely λ with lowest cost.** For each simulator, we identify the set of $\{\lambda_{\text{sim-}j}\}$, which yield policies that meet $r_{h_{\text{sim-}j}}^{\text{opt}} + \epsilon$, and select the λ whose policy has the least expected cost. Then, we identify the most common value across simulators. While the set of values here is a subset of the selection strategy A, a cost-aware selection strategy may identify a parameter that leads to a lower cost for new decision-makers.
- C. **Conservative λ .** For each simulator, we identify $\lambda_{\text{sim-}j}$ which is the minimum parameter that meets $r_{h_{\text{sim-}j}}^{\text{opt}} + \epsilon$. We then take $\max_j \lambda_{\text{sim-}j}$ over all simulated decision-makers. In the absence of suitable population-level information, this strategy is similar to picking a conservative value of λ that prioritizes performance.

We note further considerations for evaluating our proposed strategy in Appendix B.4.

5 Experimental Set-up

We now describe the experimental details for both the computational experiments in Section 6 and human subject experiments in Section 7.

5.1 Overview of Algorithms, Datasets, and Other Parameters

Algorithms and Baselines. We instantiate our algorithms, THREAD-LinUCB and THREAD-KNN, as discussed in Section 4. We provide experiments that vary algorithm-specific parameters in Section 6. We also compare against the following baselines:⁴

Human and Support, where the decision-maker *always* receives the same form of support: $\pi(x) = A_i$ for all x . As in most real-world settings, there may be an action in \mathcal{A} that corresponds to providing no support.

Population-level, where we assume we have access to learned decision support policies for m decision-makers in the population. At inference time, the decision support policy for our new decision-maker selects an arm based on the majority vote from the m policies. Depending on the task (per Section 5.2), we use populations of synthetic or real decision-makers.

⁴In Appendix A, we discuss why most prior work does not apply to our online learning setting.

Datasets. We perform computational experiments on three datasets:

1. A *Synthetic* classification task consisting of well-defined, separable clusters.
2. *CIFAR-10* [35], a 10-class image classification dataset. We describe how various subsets of the 10 classes are used in different experiments in the subsequent section.
3. *MMLU* [36], a multi-task text-based dataset, where we select four topics (math, foreign policy, biology, and computer science) that span a variety of topics.

Since the dimensionality of these image and text datasets is high, we extract lower-dimensional embeddings to help scrutinize what the decision support policy has learned. For our experiments, we use two-dimensional embeddings generated by running t-SNE [37] on the respective model embeddings for visualization purposes in human subject experiments. We provide experiments with higher dimensions in Appendix C along with how we generated these embeddings.

Number of Interactions. The number of interactions T affects how well we can estimate each r_{A_i} : the more interactions, the better our estimates using **THREAD**. In traditional online learning, T is usually unreasonably large, on the order of thousands [14, 29]. To learn personalized decision support policy in practice, we need to use more realistic values of T to account for the constraints of working with real humans (e.g., limited attention and cognitive load). In pilot studies on our tasks, we found that 60-100 interactions were a reasonable number of decisions for users to make within 20-40 minutes (a typical amount of time for an online study). We use this number of interactions for both our computational and human subject experiments, where each participant is asked to make decisions on 100 CIFAR images or 60 MMLU questions in random order.

Choice of ϵ . Along with the costs that we define for each task in Section 5.2, the choice of ϵ is a problem-specific parameter. In our experiments, we consider a tolerance value $\epsilon = 0.05$, as it is a common confidence interval.

Size of $|\mathcal{A}|$. For each task, we need to instantiate the set of support \mathcal{A} available to the decision-maker. We let kA denote when there are k forms of support. Here, we focus on support sets of size two and three; this captures a buffet of real-world scenarios in prior work where decision-makers have a few tools at their disposal to leverage as or when appropriate as discussed in Appendix A. We note that higher set sizes may also be problematic for two reasons: 1) decision-makers may struggle under many forms of support [38], and 2) as the size of $|\mathcal{A}|$ increases, we also expect the number of interactions required to learn a policy to increase.

5.2 Decision-making Tasks

We consider four tasks in our computational and human subject experiment sections. Two of the tasks are intended to provide a diversity of tasks for the computational section; the others are designed to be accessible to crowdworkers and will also be featured in the human subject experiments of Section 7.

5.2.1 Computational Only

Two tasks (Synthetic-2A and CIFAR-2A) are used only in the computational experiments so we describe them abstractly.

Synthetic-2A/CIFAR-2A. Both have the same set-up, but have different underlying data generating distributions. Consider learning a decision support policy in a setting where there are *two* forms of support available: $\mathcal{A} = \{A_1, A_2\}$, hence CIFAR-2A. Let $c(A_1) = 0$ and $c(A_2) = 0.5$. We simulate a decision-maker’s behavior under each r_{A_i} across 3 classes for Synthetic/CIFAR. We instantiate the m decision-makers in the population data using human simulations, where we randomly sample $r_{A_i}(x; h)$ from a distribution for each h in the population.

5.2.2 Computational and HSE Tasks

We also construct two tasks (CIFAR-3A and “in-the-wild” MMLU-2A) that are accessible to crowdworkers that will also be used in our human subject experiments. We construct human simulators for both tasks using estimated $\hat{r}_{A_i}(x; h)$ from real humans. We describe how we obtain estimates for $\hat{r}_{A_i}(x; h)$ from real humans for both tasks in Appendix D.4. We now overview how we instantiate the tasks and the corresponding forms of support:

CIFAR-3A. We instantiate the three-arm setting for CIFAR, as described in Appendix C. The three forms of support are (1) HUMAN ALONE, where the human makes the decision solely based on the input; (2) MODEL, which displays an ML model’s prediction for the given input, (3) CONSENSUS, which shows a distribution over labels from approximately 50 annotators [39]. We assume the cost of HUMAN ALONE is less than the cost of using either model, and the cost of MODEL and CONSENSUS is equal. Specifically, $c(\text{HUMAN ALONE}) = 0$ and $c(\text{MODEL}) = c(\text{CONSENSUS}) = 0.5$. We construct a realistic setting in which the forms of support (here, MODEL and CONSENSUS) have different strengths and weaknesses, necessitating that a decision-maker appropriately calibrate when to rely on each. We also deliberately corrupt images of different classes to evoke performance differences when they are presented to the user (see Appendix D.2 for further discussion of our set-up).

“In-the-Wild” MMLU-2A. We instantiate the two-arm setting from Table 1. The two forms of support are: HUMAN ALONE and LLM, where the human is provided responses generated from InstructGPT3.5 (text-davinci-003) [40] using the same few-shot prompting scheme for MMLU as proposed in [36]. Again, the cost of MODEL is greater than the cost of HUMAN ALONE: $c(\text{HUMAN ALONE}) = 0$ and $c(\text{MODEL}) = 0.1$. There are many topics in MMLU; to select a subset, we conducted pilots to identify where the LLM’s and average human accuracies vary, as detailed in Appendix D.3. We emphasize that the MMLU task is our “in-the-wild” evaluation because we expect people to be good at different types of topics (e.g., some people are better at foreign policy questions, but struggle in biology and computer science), akin to real-world settings where decision-makers may have differing expertise. Success on this task would indicate that THREAD can learn policies for new decision-makers online.

6 Computational Experiments

We study THREAD in a simulation-based setting where we can try multiple hyperparameters for a given decision-maker using the following workflow: For a given human, dataset, and THREAD algorithm, we use that algorithm to learn a policy with every $\lambda \in [0, 1]$ in increments of 0.05. We then select the λ that yields a policy with the lowest risk within ϵ of the Best Risk (i.e, optimal loss r_h^{opt}) of the given human. If no λ leads to a policy within ϵ of the Best Risk, we simply pick the λ corresponding to the policy with the lowest risk.

Comparison against baselines. Across the four tasks described in Section 5.2, we find that THREAD generally obtains a policy that is within $\epsilon = 0.05$ of the theoretical Best Risk but at a lower cost than baselines as shown in Table 1. For Synthetic-2A and CIFAR-2A, we find that the

Table 1: We report the expected loss $r_h(\pi)$ and the expected cost $c(\pi)$ —for both metrics, lower is better—averaged across the last 10 steps of 100 total time steps along with their standard deviations (across 5 runs) for various human simulators instantiated using synthetic and real data. For Synthetic-2A and CIFAR-2A, we learn policies for synthetic humans, whose risks are denoted in Table 1. For CIFAR-3A and MMLU-2A, we learn policies for three individuals from the observed population per Appendix D.4: the decision-maker with the lowest risk on their own (i.e., without support), the decision-maker with the lowest Best Risk, and the decision-maker with the highest Best Risk. We report the values of λ selected for each person in Table 3. We **bold** the algorithm that achieves the lowest cost within ϵ risk of the Best Risk for each human simulator, and find that our algorithm outperforms baselines on various simulated humans. For **THREAD**, we select the best policy over a sweep of λ values that minimizes Eq. 6 under $\epsilon = 0.05$.

| Synthetic Population | | | | | | | |
|----------------------|---------------------|--|--------------------|--|--------------------|---|--------------------|
| Algorithm | | $r_{A_1} = [0.7, 0.1, 0.7]$ $r_{A_2} = [0.1, 0.1, 0.1]$ | | $r_{A_1} = [0.7, 0.1, 0.7]$ $r_{A_2} = [0.1, 0.7, 0.1]$ | | $r_{A_1} = [0.7, 0.1, 0.7]$ $r_{A_2} = [0.7, 0.7, 0.1]$ | |
| | | $r_h(\pi)$ | $c(\pi)$ | $r_h(\pi)$ | $c(\pi)$ | $r_h(\pi)$ | $c(\pi)$ |
| Synthetic-2A | A ₁ Only | 0.51 ± 0.05 | 0.0 | 0.50 ± 0.06 | 0.0 | 0.50 ± 0.06 | 0.0 |
| | A ₂ Only | 0.10 ± 0.03 | 0.5 | 0.30 ± 0.05 | 0.5 | 0.50 ± 0.04 | 0.5 |
| | Population | 0.37 ± 0.04 | 0.13 ± 0.03 | 0.34 ± 0.05 | 0.13 ± 0.02 | 0.49 ± 0.06 | 0.12 ± 0.03 |
| | THREAD-LinUCB | 0.15 ± 0.05 | 0.31 ± 0.03 | 0.12 ± 0.04 | 0.32 ± 0.03 | 0.34 ± 0.11 | 0.28 ± 0.07 |
| | THREAD-KNN | 0.11 ± 0.04 | 0.36 ± 0.03 | 0.13 ± 0.04 | 0.30 ± 0.03 | 0.33 ± 0.06 | 0.21 ± 0.03 |
| | Best Risk | 0.1 | 0.33 | 0.1 | 0.33 | 0.3 | 0.17 |
| Human Population | | | | | | | |
| Algorithm | | Best alone $r_{H-ONLY} = [0.0, 0.8, 0.7, 0.3, 0.2]$ $r_{H-MODEL} = [0.0, 0.4, 0.2, 0.6, 0.6]$ $r_{H-CONSENSUS} = [0.0, 1.0, 0.4, 0.0, 0.0]$ | | Lowest best risk $r_{H-ONLY} = [0.0, 0.3, 0.7, 0.8, 0.9]$ $r_{H-MODEL} = [0.0, 0.0, 0.0, 1.0, 1.0]$ $r_{H-CONSENSUS} = [0.1, 0.6, 0.7, 0.1, 0.1]$ | | Highest best risk $r_{H-ONLY} = [0.0, 0.7, 0.9, 0.7, 0.4]$ $r_{H-MODEL} = [0.0, 0.7, 0.3, 0.7, 0.8]$ $r_{H-CONSENSUS} = [0.0, 0.6, 0.7, 0.3, 0.4]$ | |
| | | $r_h(\pi)$ | $c(\pi)$ | $r_h(\pi)$ | $c(\pi)$ | $r_h(\pi)$ | $c(\pi)$ |
| CIFAR-3A | H-ONLY | 0.42 ± 0.05 | 0.0 | 0.52 ± 0.06 | 0.0 | 0.54 ± 0.05 | 0.0 |
| | H-MODEL Only | 0.33 ± 0.05 | 0.5 | 0.41 ± 0.05 | 0.5 | 0.50 ± 0.05 | 0.5 |
| | H-CONSENSUS Only | 0.27 ± 0.03 | 0.5 | 0.41 ± 0.06 | 0.5 | 0.40 ± 0.04 | 0.5 |
| | Population | 0.42 ± 0.05 | 0.01 ± 0.01 | 0.54 ± 0.03 | 0.01 ± 0.01 | 0.53 ± 0.05 | 0.01 ± 0.01 |
| | THREAD-LinUCB | 0.23 ± 0.06 | 0.34 ± 0.08 | 0.21 ± 0.08 | 0.38 ± 0.08 | 0.43 ± 0.09 | 0.32 ± 0.08 |
| | THREAD-KNN | 0.21 ± 0.05 | 0.32 ± 0.07 | 0.11 ± 0.03 | 0.39 ± 0.03 | 0.37 ± 0.05 | 0.28 ± 0.05 |
| | Best Risk | 0.12 | 0.4 | 0.06 | 0.4 | 0.32 | 0.3 |
| Human Population | | | | | | | |
| Algorithm | | Best alone $r_{H-ONLY} = [0.3, 0.1, 0.5, 0.3]$ $r_{H-LLM} = [0.5, 0.1, 0.0, 0.1]$ | | Lowest best risk $r_{H-ONLY} = [0.3, 0.9, 0.3, 0.9]$ $r_{H-LLM} = [0.0, 0.1, 0.0, 0.3]$ | | Highest best risk $r_{H-ONLY} = [0.8, 0.6, 0.8, 0.6]$ $r_{H-LLM} = [0.6, 0.3, 0.7, 0.1]$ | |
| | | $r_h(\pi)$ | $c(\pi)$ | $r_h(\pi)$ | $c(\pi)$ | $r_h(\pi)$ | $c(\pi)$ |
| MMLU-2A | H-ONLY | 0.30 ± 0.03 | 0.0 | 0.54 ± 0.05 | 0.0 | 0.68 ± 0.03 | 0.0 |
| | H-LLM Only | 0.21 ± 0.03 | 0.1 | 0.09 ± 0.02 | 0.1 | 0.42 ± 0.06 | 0.1 |
| | Population | 0.13 ± 0.03 | 0.05 ± 0.01 | 0.35 ± 0.07 | 0.05 ± 0.01 | 0.53 ± 0.05 | 0.05 ± 0.01 |
| | THREAD-LinUCB | 0.15 ± 0.05 | 0.04 ± 0.01 | 0.20 ± 0.10 | 0.05 ± 0.02 | 0.51 ± 0.06 | 0.06 ± 0.01 |
| | THREAD-KNN | 0.17 ± 0.03 | 0.03 ± 0.01 | 0.12 ± 0.03 | 0.08 ± 0.01 | 0.46 ± 0.05 | 0.06 ± 0.01 |
| | Best Risk | 0.13 | 0.08 | 0.09 | 0.1 | 0.42 | 0.1 |

two variants are comparable in terms of expected risk and cost. For CIFAR-3A and MMLU-2A, we find that **THREAD-KNN** generally outperforms **THREAD-LinUCB** for all three individuals. For the individual who performs the best alone, we find that **THREAD-KNN**, **THREAD-LinUCB**, and the Population baseline are all within ϵ of the Best Risk; however, **THREAD-KNN** is the cheapest.

For most individuals, the population baseline performs poorly, suggesting that there is likely misalignment between the population policy and the optimal policy of the new decision-maker (i.e., the individual has different prediction errors $r_{A_i}(x; h)$ than the individuals in the population). There are only a few individuals for whom the population policy yields an appropriate amount of

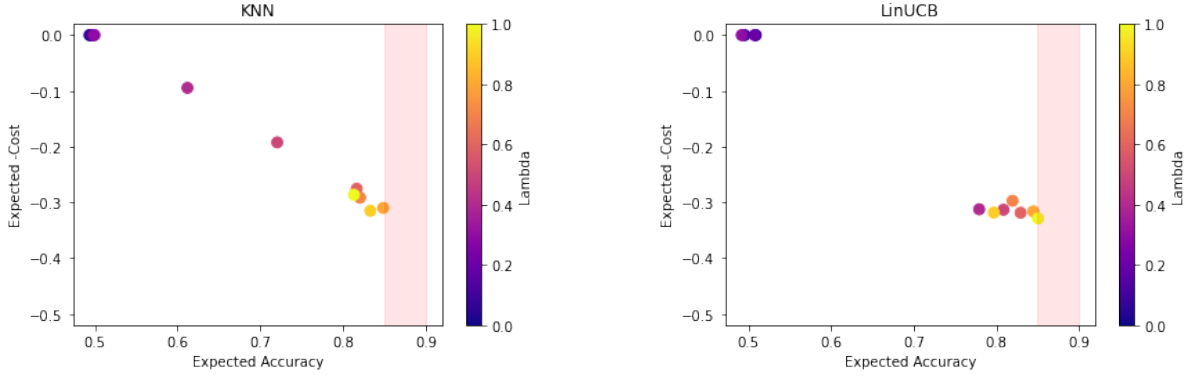


Figure 3: We plot the expected accuracy and the negative of the expected cost for an individual sampled from the Synthetic-2A dataset for $\lambda \in [0, 1]$. The ideal policy would lie in the far right corner. The red region denotes policies that fall within ϵ of the best risk for the sampled individual. We observe that there exists a policy that lies in the red region for both **THREAD-KNN** and **THREAD-LinUCB**.

excess risk (e.g., the MMLU-2A decision-maker who is best without support). See Appendix B.3 for additional discussion. Future work could extend **THREAD** to fine-tune a population baseline for a new decision-maker.

Effect of problem- and algorithm-specific parameters. We explore the effect of misspecification that may arise due to selecting the wrong value of the trade-off parameter λ . Consider Figure 3 which are generated plots for both **THREAD-KNN** and **THREAD-LinUCB**. We can see that only a subset of λ values fall within the red band (i.e., within $\epsilon = 0.05$ of the Best Risk of that individual), suggesting the importance of selecting an appropriate value of λ . We also observe that as λ increases, **THREAD-KNN** has more monotonic and controllable behavior. In contrast, λ seems to have less of an effect on **THREAD-LinUCB**. We evaluate whether similar observations hold in our subsequent human subject experiments.

While we have focused on selecting an appropriate problem-specific hyperparameter λ , we also explore the effect of algorithm-specific hyperparameters. When we vary the exploration parameters of the two online learning algorithms, we find in Table 4 that increasing the amount of exploration leads to better performance for **THREAD-LinUCB**, and decreasing the amount of exploration leads to better performance for **THREAD-KNN**. We vary KNN parameters in Table 5: over multiple datasets, we find that the average loss tends to increase as the number of neighbors K gets larger, and the average cost increases as the warm-up period W gets larger. We advise future work on deploying **THREAD** for new datasets to consider running similar ablation experiments with human simulators to understand the different trends for algorithm-specific hyperparameters.

7 Human Subject Validation

To validate whether our decision support policies learned via **THREAD** work in practice, we run human subject experiments (HSE) – extending our computational evaluations in a series of ethics-reviewed studies with real human participants. As we overview in Appendix A, prior work does not run user studies that personalize policies online. Here, we *do* learn policies for individual humans on two tasks for our HSEs. We first discuss how we translated the computational set-up into HSEs and then present the results.

7.1 User study details

Interactive Interface. To translate our problem formulation and decision support algorithm into an interactive tool, we create **Modiste**, which provides an interface for **THREAD**. At each time

step, **Modiste** sends each user’s predictions to a backend server, running **THREAD**, which identifies the next form of support for the next input. **Modiste** then updates the interface accordingly to reflect the selected form of support. As we demonstrate, our tool can flexibly be linked with crowdsourcing platforms like Prolific [41]. We provide screenshots of the interface under each form of support in Appendix D, as well as the algorithm parameters used to initialize **THREAD**. Participants are informed of their own correctness after each trial, as well as the correctness of the form of support (e.g., ML model), if support was provided; we choose to reveal correctness after each trial such that the participant can learn whether or not support ought to be relied upon (see Appendix D for a preliminary analysis of participant reliance).

Recruitment Details. We recruit a total of 125 crowdsourced participants from Prolific [41] to interact with **Modiste** (N=45 and 80 for the CIFAR and MMLU tasks, respectively). We recruit more participants for MMLU, as we expect greater individual differences in regions where support is needed, e.g., some participants may be good at mathematics and struggle in biology, whereas others may excel in biology questions, whereas in CIFAR, there is an “optimal” form of support for each stimulus. Each participant is assigned to only one task and one algorithm. Further details are provided in Appendix D.

Trade-off Parameter Selection. We follow the strategies specified in Section 4.2 to identify trade-off parameters for our HSEs, i.e., using population data collected per Appendix D.4. We visualize this process in further detail in Figure 7. For CIFAR, the parameter values for LinUCB were $\lambda_A = 0.85, \lambda_B = 0.85, \lambda_C = 1.0$ and for KNN were $\lambda_A = 0.75, \lambda_B = 0.75, \lambda_C = 1.0$. For MMLU, the parameter values for LinUCB were $\lambda_A = 1.0, \lambda_B = 0.95, \lambda_C = 1.0$ and for KNN were $\lambda_A = 0.65, \lambda_B = 0.75, \lambda_C = 0.9$.

7.2 Results

THREAD balances performance and cost. In Figure 4, we present participants’ attained accuracy (inverted expected risk) and inverted cost (per Eq. 1 and Eq. 2 respectively) on **THREAD** as well as baselines.⁵ In general, we observe the benefits of online learning for identifying low-cost yet effective support.

In both tasks, **HUMAN ALONE** leads to poor performance. Further, while relying on a fixed, population-level policy may be effective for some participants – the policy may be misaligned for participants who deviate from the population, hampering their decision making. For instance, the MMLU **POPULATION** baseline always defers on biology questions, yet, one participant continually struggled with biology questions – noting in the comments that they found this topic the most difficult. With **Modiste**, we can learn that this participant need support on biology questions and adjust the policy accordingly. Indeed, on MMLU, **Modiste** yields policies *personalized to individual users’ strengths and weaknesses* as shown in Figure 5 (Right). Specifically, LLM support was generally provided for topics where participants were weak and participants made their own decisions to save cost (i.e., selecting **HUMAN ALONE**) where they are already strong. *We learn when a participant would benefit from using an LLM and when they would not.* We observe similar personalization for **CIFAR**. In Appendix D, we visualize the final decision support policy for multiple participants under each **THREAD** variant on both tasks; here, we can also clearly see the impact of the algorithm on learned policy characteristics (e.g., LinUCB permits only linear decision boundaries, while KNN yields “spottier” policies).

Effect of reliance on support. However, **Modiste** is not uniformly successful; for some participants, an effective policy was not discovered and decision making outcomes suffered. We

⁵All participants in Population baseline receive the same form of support for a given instance; the variance over the average cost comes from randomization in the instances shown over the last 10 trials.

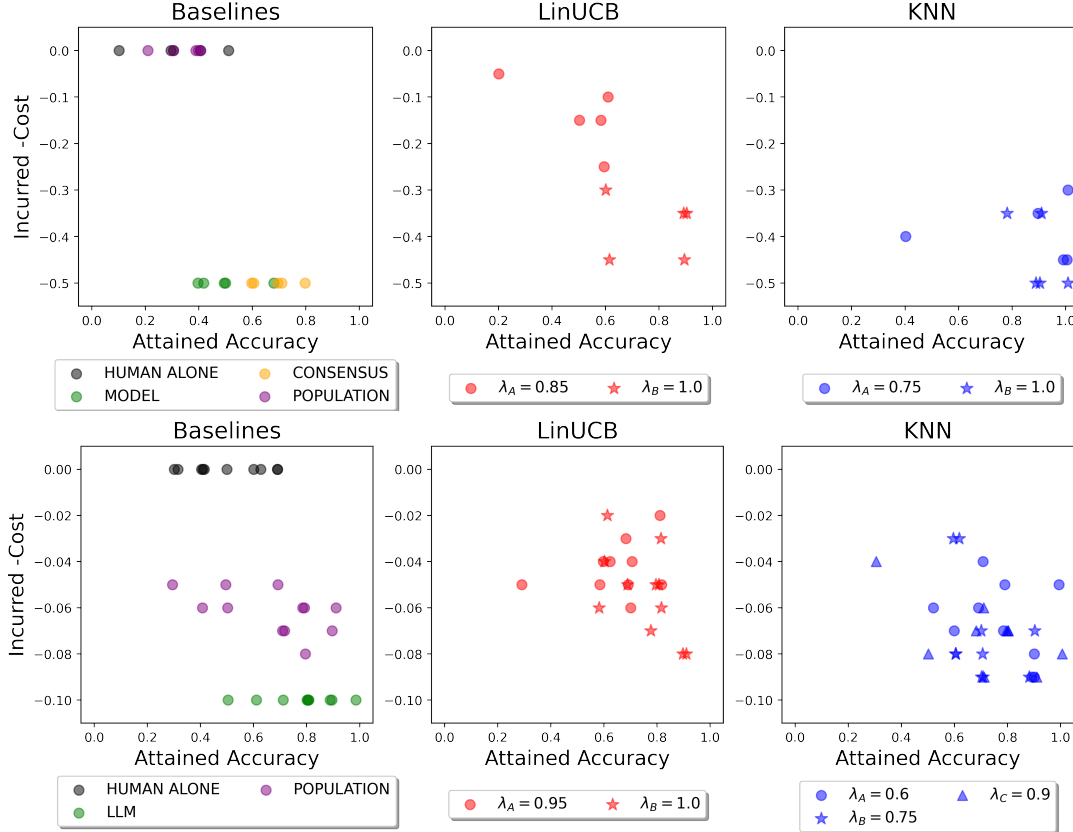


Figure 4: We compare the decision-making performance (i.e., accuracy attained) and incurred (negative) cost by Prolific participants in the last 10 trials. Each point represents a single participant. Higher accuracy and higher negative cost are better (i.e., the top right is preferred). We see that in both domains (top = CIFAR; bottom = MMLU), our algorithms tradeoff between decision-making performance and incurred cost; however, the comparative results are not as straightforward as in the computational experiments: real humans are nuanced.

hypothesize that participants who have miscalibrated degrees of reliance (e.g., failed to take into account the support of a model when it was correct, or overrelied on a model when it was incorrect) may make it harder to learn a good personal policy. To investigate, we define a measure of “reliance sensibility”: i.e., the proportion of trials the participant agreed with the support when correct and responding differently when the support was incorrect, out of all trials where the participant received support. The higher the proportion, the more “sensible” a participant’s degree of reliance on the provided support is, relative to what would be most beneficial for decision outcomes.⁶

We find in Figure 12 that in the MMLU task, there *does* seem to be a relationship between a participant’s reliance and the final average loss incurred by the learned policy (Pearson r correlation = -0.47 and -0.59 for KNN and LinUCB, respectively). In the CIFAR task, we note that participants largely had calibrated reliance, and such reliance was not a strong predictor of incurred loss for KNN (Pearson $r = -0.1$), though may be for LinUCB (Pearson $r = -0.64$) albeit the minimal variance in reliance obfuscates the possible relationship.

Comparing simulations and HSEs. Additionally, it is important to consider the fidelity of our human simulators against the human behavior we observe in practice, as the use of human simulators is also relied upon in prior work (see Appendix). We find the impact of the trade-off

⁶Note that we cannot directly deduce whether, or to what degree, an individual participant relied on the form of support when presented - since we do not have access to what an individually would have said without support; alternative reliance inference schemes like [42] could be considered in future work.

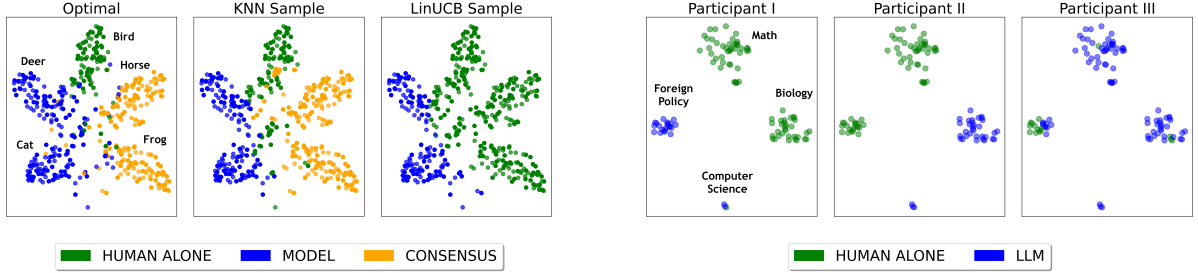


Figure 5: A snapshot of the recommended forms of support from participant policies learned via **Modiste**. Snapshots are computed at the end of a set of interactions with each individual user. The forms of support are depicted as colorings across the embedding space. Left (CIFAR): KNN leads to more optimal support decompositions compared to LinUCB. Right (MMLU): **Modiste** learns policies personalized to each participant’s strengths and weaknesses. Participant I particularly excelled at biology questions (100% accuracy by themselves), whereas Participant II never got a biology or CS question correct when unassisted; Participant III struggled on all topics with the exception of foreign policy (albeit performance by themselves was not as high as the LLM). The learned policies capture these differences – modulating the provision of support based on individuals’ educational proficiencies. Details on how these plots are generated, in addition to additional participant plots (Figures 10 and 11) are included in Appendix D.

parameter λ in the computational experiments may be overstated, as we find that performance has a lower sensitivity to λ in the HSEs; unlike in Figure 4, choice of λ has minimal impact on the quality of learned policies for real humans. This disconnect underscores that, despite grounding human simulations in real data, there remain assumptions about the human simulations which deviate from real user behavior, e.g., accounting for varied reliance strategies. We suggest future algorithms for learning decision support policies consider accounting for human idiosyncrasies, irregularities, and uncertainty [43].

8 Conclusion

A decision support policy captures when and which form of support should be provided to improve a decision-maker’s performance. To the best of our knowledge, we are the first to consider learning this policy online. For decision-makers about whom we have no information, we solve a multi-objective optimization problem that trades off performance and cost. We propose **THREAD**, an algorithm for learning a decision support policy for a given trade-off parameter that modulates cost and performance, and instantiate two variants of **THREAD** using stochastic contextual bandits. We introduce a hyper-parameter tuning strategy that uses **THREAD** to find a trade-off parameter, which meets a specified performance threshold for simulated decision-makers and can be used to deploy **THREAD** on real decision-maker. We develop **Modiste**, an interactive tool that provides an interface for **THREAD** to be used in practice. We perform computational and human subject experiments to highlight the importance – and feasibility – of personalizing decision support policies to individual decision-makers. Our human subject experiments thrillingly show the usefulness of **Modiste** to learn decision support policies in remarkably few iterations and to tease apart differences in decision-makers’ need for support. Future work can integrate complex algorithms into **THREAD** to handle potential drifts in decision-maker behavior and can use **Modiste** to tailor decision support policies in deployed real-world settings.

Acknowledgements

UB acknowledges support from DeepMind and the Leverhulme Trust via the Leverhulme Centre for the Future of Intelligence (CFI). AW acknowledges support from a Turing AI Fellowship under grant EP/V025279/1, EPSRC grants EP/V056522/1 and EP/V056883/1, and the Leverhulme

Trust via CFI. KMC acknowledges support from a Marshall Scholarship and the Cambridge Trust. PK acknowledges support from The Alan Turing Institute. AT acknowledges support from the National Science Foundation grants IIS1705121, IIS1838017, IIS2046613, IIS2112471, an Amazon Web Services Award, a Facebook Faculty Research Award, funding from Booz Allen Hamilton Inc., and a Block Center Grant. Any opinions, findings and conclusions or recommendations expressed in this material are those of the author(s) and do not necessarily reflect the views of any of these funding agencies. We thank the Prolific participants who took part in our studies, as well as our Cambridge-based volunteer pilot participants. We thank Alan Liu and Kartik Chandra for their invaluable input on designing our web-based server.

References

- [1] Peter GW Keen. Decision support systems: a research perspective. In *Decision support systems: Issues and challenges: Proceedings of an international task force meeting*, pages 23–44, 1980.
- [2] Charles E Kahn Jr. Artificial intelligence in radiology: decision support systems. *Radio-graphics*, 14(4):849–861, 1994.
- [3] Gavin M Briggs, Peter A Flynn, M Worthington, I Rennie, and CS McKinstry. The role of specialist neuroradiology second opinion reporting: is there added value? *Clinical radiology*, 63(7):791–795, 2008.
- [4] Tom B. Brown, Benjamin Mann, Nick Ryder, Melanie Subbiah, Jared Kaplan, Prafulla Dhariwal, Arvind Neelakantan, Pranav Shyam, Girish Sastry, Amanda Askell, Sandhini Agarwal, Ariel Herbert-Voss, Gretchen Krueger, Tom Henighan, Rewon Child, Aditya Ramesh, Daniel M. Ziegler, Jeffrey Wu, Clemens Winter, Christopher Hesse, Mark Chen, Eric Sigler, Mateusz Litwin, Scott Gray, Benjamin Chess, Jack Clark, Christopher Berner, Sam McCandlish, Alec Radford, Ilya Sutskever, and Dario Amodei. Language models are few-shot learners. *CoRR*, abs/2005.14165, 2020. URL <https://arxiv.org/abs/2005.14165>.
- [5] Rishi Bommasani, Drew A. Hudson, Ehsan Adeli, Russ B. Altman, Simran Arora, Sydney von Arx, Michael S. Bernstein, Jeannette Bohg, Antoine Bosselut, Emma Brunskill, Erik Brynjolfsson, Shyamal Buch, Dallas Card, Rodrigo Castellon, Niladri S. Chatterji, Annie S. Chen, Kathleen Creel, Jared Quincy Davis, Dorottya Demszky, Chris Donahue, Moussa Doumbouya, Esin Durmus, Stefano Ermon, John Etchemendy, Kawin Ethayarajh, Li Fei-Fei, Chelsea Finn, Trevor Gale, Lauren Gillespie, Karan Goel, Noah D. Goodman, Shelby Grossman, Neel Guha, Tatsunori Hashimoto, Peter Henderson, John Hewitt, Daniel E. Ho, Jenny Hong, Kyle Hsu, Jing Huang, Thomas Icard, Saahil Jain, Dan Jurafsky, Pratyusha Kalluri, Siddharth Karamcheti, Geoff Keeling, Fereshte Khani, Omar Khattab, Pang Wei Koh, Mark S. Krass, Ranjay Krishna, Rohith Kuditipudi, and et al. On the opportunities and risks of foundation models. *CoRR*, abs/2108.07258, 2021. URL <https://arxiv.org/abs/2108.07258>.
- [6] Karan Singhal, Shekoofeh Azizi, Tao Tu, S Sara Mahdavi, Jason Wei, Hyung Won Chung, Nathan Scales, Ajay Tanwani, Heather Cole-Lewis, Stephen Pfohl, et al. Large language models encode clinical knowledge. *arXiv preprint arXiv:2212.13138*, 2022.
- [7] Qian Yang, Yuexing Hao, Kexin Quan, Stephen Yang, Yiran Zhao, Volodymyr Kuleshov, and Fei Wang. Harnessing biomedical literature to calibrate clinicians’ trust in ai decision support systems. 04 2023. doi: 10.1145/3544548.3581393.

- [8] Zoya K Arbiser, Andrew L Folpe, and Sharon W Weiss. Consultative (expert) second opinions in soft tissue pathology: analysis of problem-prone diagnostic situations. *American journal of clinical pathology*, 116(4):473–476, 2001.
- [9] Wanda Mimra, Alexander Rasch, and Christian Waibel. Second opinions in markets for expert services: Experimental evidence. *Journal of Economic Behavior & Organization*, 131:106–125, 2016.
- [10] Cassidy Laidlaw and Stuart Russell. Uncertain decisions facilitate better preference learning. *Advances in Neural Information Processing Systems*, 34:15070–15083, 2021.
- [11] Mohammad-Amin Charusaie, Hussein Mozannar, David Sontag, and Samira Samadi. Sample efficient learning of predictors that complement humans. In *International Conference on Machine Learning*, pages 2972–3005. PMLR, 2022.
- [12] Maria De-Arteaga, Artur Dubrawski, and Alexandra Chouldechova. Learning under selective labels in the presence of expert consistency. *arXiv preprint arXiv:1807.00905*, 2018.
- [13] Hussein Mozannar and David Sontag. Consistent estimators for learning to defer to an expert. In *International Conference on Machine Learning*, pages 7076–7087. PMLR, 2020.
- [14] Lihong Li, Wei Chu, John Langford, and Robert E Schapire. A contextual-bandit approach to personalized news article recommendation. In *Proceedings of the 19th international conference on World wide web*, pages 661–670, 2010.
- [15] Richard T Scheife, Lisa E Hines, Richard D Boyce, Sophie P Chung, Jeremiah D Momper, Christine D Sommer, Darrell R Abernethy, John R Horn, Stephen J Sklar, Samantha K Wong, et al. Consensus recommendations for systematic evaluation of drug–drug interaction evidence for clinical decision support. *Drug safety*, 38(2):197–206, 2015.
- [16] Claudia Ed Roda. *Human attention and its implications for human-computer interaction*. Cambridge University Press, 2011.
- [17] Gloria Phillips-Wren. Ai tools in decision making support systems: a review. *International Journal on Artificial Intelligence Tools*, 21(02):1240005, 2012.
- [18] Ruijiang Gao, Maytal Saar-Tsechansky, Maria De-Arteaga, Ligong Han, Min Kyung Lee, and Matthew Lease. Human-AI collaboration with bandit feedback. In *Proceedings of the Thirtieth International Joint Conference on Artificial Intelligence, IJCAI-21*, pages 1722–1728. International Joint Conferences on Artificial Intelligence Organization, 2021.
- [19] David Madras, Toni Pitassi, and Richard Zemel. Predict responsibly: improving fairness and accuracy by learning to defer. *Advances in Neural Information Processing Systems*, 31, 2018.
- [20] Vijay Keswani, Matthew Lease, and Krishnaram Kenthapadi. Towards unbiased and accurate deferral to multiple experts. In *Proceedings of the 2021 AAAI/ACM Conference on AI, Ethics, and Society*, pages 154–165, 2021.
- [21] Patrick Hemmer, Sebastian Schellhammer, Michael Vössing, Johannes Jakubik, and Gerhard Satzger. Forming effective human-AI teams: Building machine learning models that complement the capabilities of multiple experts. In *Proceedings of the Thirtieth International Conference on International Joint Conferences on Artificial Intelligence*, 2022.
- [22] Ben Green and Yiling Chen. The principles and limits of algorithm-in-the-loop decision making. *Proceedings of the ACM on Human-Computer Interaction*, 3(CSCW):1–24, 2019.

- [23] Vivian Lai, Chacha Chen, Q Vera Liao, Alison Smith-Renner, and Chenhao Tan. Towards a science of human-ai decision making: a survey of empirical studies. *arXiv preprint arXiv:2112.11471*, 2021.
- [24] Gagan Bansal, Tongshuang Wu, Joyce Zhou, Raymond Fok, Besmira Nushi, Ece Kamar, Marco Tulio Ribeiro, and Daniel Weld. Does the whole exceed its parts? The effect of AI explanations on complementary team performance. In *Proceedings of the 2021 CHI Conference on Human Factors in Computing Systems*, pages 1–16, 2021.
- [25] Yunfeng Zhang, Q Vera Liao, and Rachel KE Bellamy. Effect of confidence and explanation on accuracy and trust calibration in ai-assisted decision making. In *Proceedings of the 2020 conference on fairness, accountability, and transparency*, pages 295–305, 2020.
- [26] Varun Babbar, Umang Bhatt, and Adrian Weller. On the utility of prediction sets in human-ai teams. In Lud De Raedt, editor, *Proceedings of the Thirty-First International Joint Conference on Artificial Intelligence, IJCAI-22*, pages 2457–2463. International Joint Conferences on Artificial Intelligence Organization, 7 2022. Main Track.
- [27] Nastaran Okati, Abir De, and Manuel Rodriguez. Differentiable learning under triage. *Advances in Neural Information Processing Systems*, 34:9140–9151, 2021.
- [28] Ruijiang Gao, Maytal Saar-Tsechansky, Maria De-Arteaga, Ligong Han, Wei Sun, Min Kyung Lee, and Matthew Lease. Learning complementary policies for human-ai teams. *arXiv preprint arXiv:2302.02944*, 2023.
- [29] Melody Guan and Heinrich Jiang. Nonparametric stochastic contextual bandits. In *Proceedings of the AAAI Conference on Artificial Intelligence*, volume 32, 2018.
- [30] Cem Tekin and Eralp Turgay. Multi-objective contextual multi-armed bandit with a dominant objective. *IEEE Transactions on Signal Processing*, 66(14):3799–3813, 2018.
- [31] Eralp Turgay, Doruk Oner, and Cem Tekin. Multi-objective contextual bandit problem with similarity information. In *International Conference on Artificial Intelligence and Statistics*, pages 1673–1681. PMLR, 2018.
- [32] Andreu Mas-Colell, Michael Dennis Whinston, Jerry R Green, et al. *Microeconomic theory*, volume 1. Oxford university press New York, 1995.
- [33] Jurgen Branke, Jürgen Branke, Kalyanmoy Deb, Kaisa Miettinen, and Roman Slowiński. *Multiobjective optimization: Interactive and evolutionary approaches*, volume 5252. Springer Science & Business Media, 2008.
- [34] Choong Nyoung Kim, Kyung Hoon Yang, and Jaekyung Kim. Human decision-making behavior and modeling effects. *Decision Support Systems*, 45(3):517–527, 2008.
- [35] Alex Krizhevsky. Learning multiple layers of features from tiny images. *Master’s thesis, University of Toronto*, 2009.
- [36] Dan Hendrycks, Collin Burns, Steven Basart, Andy Zou, Mantas Mazeika, Dawn Song, and Jacob Steinhardt. Measuring massive multitask language understanding. In *International Conference on Learning Representations*, 2020.
- [37] Laurens Van der Maaten and Geoffrey Hinton. Visualizing data using t-sne. *Journal of machine learning research*, 9(11), 2008.
- [38] Annemarie Kalis, Stefan Kaiser, and Andreas Mojzisch. Why we should talk about option generation in decision-making research. *Frontiers in psychology*, 4:555, 2013.

- [39] Joshua C Peterson, Ruairidh M Battleday, Thomas L Griffiths, and Olga Russakovsky. Human uncertainty makes classification more robust. In *Proceedings of the IEEE/CVF International Conference on Computer Vision*, pages 9617–9626, 2019.
- [40] Long Ouyang, Jeff Wu, Xu Jiang, Diogo Almeida, Carroll L. Wainwright, Pamela Mishkin, Chong Zhang, Sandhini Agarwal, Katarina Slama, Alex Ray, John Schulman, Jacob Hilton, Fraser Kelton, Luke Miller, Maddie Simens, Amanda Askell, Peter Welinder, Paul Christiano, Jan Leike, and Ryan Lowe. Training language models to follow instructions with human feedback, 2022. URL <https://arxiv.org/abs/2203.02155>.
- [41] Stefan Palan and Christian Schitter. Prolific. ac—a subject pool for online experiments. *Journal of Behavioral and Experimental Finance*, 17:22–27, 2018.
- [42] Heliodoro Tejada, Aakriti Kumar, Padhraic Smyth, and Mark Steyvers. Ai-assisted decision-making: A cognitive modeling approach to infer latent reliance strategies. *Computational Brain & Behavior*, pages 1–18, 2022.
- [43] Mark Steyvers and Aakriti Kumar. Three challenges for ai-assisted decision-making. 2022.
- [44] Corinna Cortes, Giulia DeSalvo, and Mehryar Mohri. Learning with rejection. In *International Conference on Algorithmic Learning Theory*, pages 67–82. Springer, 2016.
- [45] Corinna Cortes, Giulia DeSalvo, Claudio Gentile, Mehryar Mohri, and Scott Yang. Online learning with abstention. In *International conference on machine learning*, pages 1059–1067. PMLR, 2018.
- [46] Vladimir Vovk. A game of prediction with expert advice. *Journal of Computer and System Sciences*, 56(2):153–173, 1998.
- [47] Hussein Mozannar, Arvind Satyanarayan, and David Sontag. Teaching humans when to defer to a classifier via exemplars. In *Proceedings of the AAAI Conference on Artificial Intelligence*, volume 36, pages 5323–5331, 2022.
- [48] Vivian Lai, Samuel Carton, Rajat Bhatnagar, Q Vera Liao, Yunfeng Zhang, and Chenhao Tan. Human-AI collaboration via conditional delegation: A case study of content moderation. In *CHI Conference on Human Factors in Computing Systems*, pages 1–18, 2022.
- [49] Sebastian Bordt and Ulrike Von Luxburg. A bandit model for human-machine decision making with private information and opacity. In *International Conference on Artificial Intelligence and Statistics*, pages 7300–7319. PMLR, 2022.
- [50] Gali Noti and Yiling Chen. Learning when to advise human decision makers. *arXiv preprint arXiv:2209.13578*, 2022.
- [51] Nicholas Wolczynski, Maytal Saar-Tsechansky, and Tong Wang. Learning to advise humans by leveraging algorithm discretion. *arXiv preprint arXiv:2210.12849*, 2022.
- [52] Gagan Bansal, Besmira Nushi, Ece Kamar, Eric Horvitz, and Daniel S Weld. Is the most accurate AI the best teammate? optimizing AI for teamwork. In *Proceedings of the AAAI Conference on Artificial Intelligence*, volume 35, pages 11405–11414, 2021.
- [53] Bryan Wilder, Eric Horvitz, and Ece Kamar. Learning to complement humans. In *Proceedings of the Twenty-Ninth International Conference on International Joint Conferences on Artificial Intelligence*, pages 1526–1533, 2021.

- [54] Chi-Keung Chow. An optimum character recognition system using decision functions. *IRE Transactions on Electronic Computers*, (4):247–254, 1957.
- [55] Yonatan Geifman and Ran El-Yaniv. Selective classification for deep neural networks. *Advances in neural information processing systems*, 30, 2017.
- [56] Sherry Yang, Ofir Nachum, Yilun Du, Jason Wei, Pieter Abbeel, and Dale Schuurmans. Foundation models for decision making: Problems, methods, and opportunities. *arXiv preprint arXiv:2303.04129*, 2023.
- [57] Hussein Mozannar, Gagan Bansal, Adam Fourney, and Eric Horvitz. Reading between the lines: Modeling user behavior and costs in ai-assisted programming. *arXiv preprint arXiv:2210.14306*, 2022.
- [58] Vladimir Vovk, Alex Gammerman, and Glenn Shafer. *Algorithmic Learning in a Random World*. Springer, 01 2005. doi: 10.1007/b106715.
- [59] Elizabeth Bondi, Raphael Koster, Hannah Sheahan, Martin Chadwick, Yoram Bachrach, Taylan Cemgil, Ulrich Paquet, and Krishnamurthy Dvijotham. Role of Human-AI Interaction in Selective Prediction. *Proceedings of the AAAI Conference on Artificial Intelligence*, 2022.
- [60] Stephen Bates, Anastasios Angelopoulos, Lihua Lei, Jitendra Malik, and Michael Jordan. Distribution-free, risk-controlling prediction sets. *Journal of the ACM (JACM)*, 68(6):1–34, 2021.
- [61] Eleni Straitouri, Lequn Wang, Nastaran Okati, and Manuel Gomez Rodriguez. Provably improving expert predictions with conformal prediction. *arXiv preprint arXiv:2201.12006*, 2022.
- [62] David Spiegelhalter. Risk and Uncertainty Communication. 4(1):31–60, 2017. ISSN 2326-8298, 2326-831X. doi: 10.1146/annurev-statistics-010814-020148. URL <http://www.annualreviews.org/doi/10.1146/annurev-statistics-010814-020148>.
- [63] Umang Bhatt, Javier Antorán, Yunfeng Zhang, Q. Vera Liao, Prasanna Sattigeri, Riccardo Fogliato, Gabrielle Melançon, Ranganath Krishnan, Jason Stanley, Omesh Tickoo, Lama Nachman, Rumi Chunara, Madhulika Srikumar, Adrian Weller, and Alice Xiang. Uncertainty as a Form of Transparency: Measuring, Communicating, and Using Uncertainty. In *Proceedings of the 2021 AAAI/ACM Conference on AI, Ethics, and Society*, page 401–413, New York, NY, USA, 2021. ISBN 9781450384735.
- [64] Jessica Hullman, Xiaoli Qiao, Michael Correll, Alex Kale, and Matthew Kay. In pursuit of error: A survey of uncertainty visualization evaluation. *IEEE transactions on visualization and computer graphics*, 25(1):903–913, 2018.
- [65] Marco Tulio Ribeiro, Sameer Singh, and Carlos Guestrin. " why should i trust you?" explaining the predictions of any classifier. In *Proceedings of the 22nd ACM SIGKDD international conference on knowledge discovery and data mining*, pages 1135–1144, 2016.
- [66] Zana Bućinca, Phoebe Lin, Krzysztof Z Gajos, and Elena L Glassman. Proxy tasks and subjective measures can be misleading in evaluating explainable ai systems. In *Proceedings of the 25th International Conference on Intelligent User Interfaces*, pages 454–464, 2020.
- [67] Been Kim, Cynthia Rudin, and Julie A Shah. The bayesian case model: A generative approach for case-based reasoning and prototype classification. In *Advances in neural information processing systems*, pages 1952–1960, 2014.

- [68] Jeya Vikranth Jeyakumar, Joseph Noor, Yu-Hsi Cheng, Luis Garcia, and Mani Srivastava. How can i explain this to you? an empirical study of deep neural network explanation methods. *Advances in Neural Information Processing Systems*, 33, 2020.
- [69] Berk Ustun, Alexander Spangher, and Yang Liu. Actionable recourse in linear classification. In *Proceedings of the Conference on Fairness, Accountability, and Transparency*, pages 10–19, 2019.
- [70] Javier Antoran, Umang Bhatt, Tameem Adel, Adrian Weller, and José Miguel Hernández-Lobato. Getting a clue: A method for explaining uncertainty estimates. In *International Conference on Learning Representations*, 2020.
- [71] Upol Ehsan, Brent Harrison, Larry Chan, and Mark O Riedl. Rationalization: A neural machine translation approach to generating natural language explanations. In *Proceedings of the 2018 AAAI/ACM Conference on AI, Ethics, and Society*, pages 81–87, 2018.
- [72] Oana-Maria Camburu, Tim Rocktäschel, Thomas Lukasiewicz, and Phil Blunsom. e-snli: Natural language inference with natural language explanations. *Advances in Neural Information Processing Systems*, 31, 2018.
- [73] Valerie Chen, Jeffrey Li, Joon Sik Kim, Gregory Plumb, and Ameet Talwalkar. Interpretable machine learning: Moving from mythos to diagnostics. *Queue*, 19(6):28–56, 2022.
- [74] John Zerilli, Umang Bhatt, and Adrian Weller. How transparency modulates trust in artificial intelligence. *Patterns*, page 100455, 2022.
- [75] Valerie Chen, Q Vera Liao, Jennifer Wortman Vaughan, and Gagan Bansal. Understanding the role of human intuition on reliance in human-ai decision-making with explanations. *arXiv preprint arXiv:2301.07255*, 2023.
- [76] Lucas Beyer, Olivier J. Hénaff, Alexander Kolesnikov, Xiaohua Zhai, and Aäron van den Oord. Are we done with imagenet? *CoRR*, abs/2006.07159, 2020. URL <https://arxiv.org/abs/2006.07159>.
- [77] Alexandra Uma, Dina Almanea, and Massimo Poesio. Scaling and disagreements: Bias, noise, and ambiguity. *Frontiers in Artificial Intelligence*, 5, 2022.
- [78] Alexandra Uma, Tommaso Fornaciari, Dirk Hovy, Silviu Paun, Barbara Plank, and Massimo Poesio. A case for soft loss functions. *Proceedings of the AAAI Conference on Human Computation and Crowdsourcing*, 8(1):173–177, Oct. 2020. URL <https://ojs.aaai.org/index.php/HCOMP/article/view/7478>.
- [79] Mitchell L Gordon, Kaitlyn Zhou, Kayur Patel, Tatsunori Hashimoto, and Michael S Bernstein. The disagreement deconvolution: Bringing machine learning performance metrics in line with reality. In *Proceedings of the 2021 CHI Conference on Human Factors in Computing Systems*, pages 1–14, 2021.
- [80] Mitchell L Gordon, Michelle S Lam, Joon Sung Park, Kayur Patel, Jeff Hancock, Tatsunori Hashimoto, and Michael S Bernstein. Jury learning: Integrating dissenting voices into machine learning models. In *CHI Conference on Human Factors in Computing Systems*, pages 1–19, 2022.
- [81] Katherine M Collins, Umang Bhatt, and Adrian Weller. Eliciting and learning with soft labels from every annotator. In *Proceedings of the AAAI Conference on Human Computation and Crowdsourcing (HCOMP)*, volume 10, 2022.

- [82] Katherine M. Collins, Matthew Barker, Mateo Espinosa Zarlenga, Naveen Raman, Umang Bhatt, Mateja Jamnik, Ilia Sucholutsky, Adrian Weller, and Krishnamurthy Dvijotham. Human uncertainty in concept-based ai systems, 2023.
- [83] Alexander Philip Dawid and Allan M Skene. Maximum likelihood estimation of observer error-rates using the em algorithm. *Journal of the Royal Statistical Society: Series C (Applied Statistics)*, 28(1):20–28, 1979.
- [84] Alexandry Augustin, Matteo Venanzi, Alex Rogers, and Nicholas R Jennings. Bayesian aggregation of categorical distributions with applications in crowdsourcing. In *IJCAI*, pages 1411–1417, 2017.
- [85] Jacob Whitehill, Ting-fan Wu, Jacob Bergsma, Javier Movellan, and Paul Ruvolo. Whose vote should count more: Optimal integration of labels from labelers of unknown expertise. *Advances in neural information processing systems*, 22, 2009.
- [86] Jiaheng Wei, Zhaowei Zhu, Hao Cheng, Tongliang Liu, Gang Niu, and Yang Liu. Learning with noisy labels revisited: A study using real-world human annotations. In *International Conference on Learning Representations*, 2022. URL <https://openreview.net/forum?id=TBWA6PLJZQm>.
- [87] A. O’Hagan, C. E. Buck, A. Daneshkhah, J. R. Eiser, P. H. Garthwaite, D. J. Jenkinson, J. E. Oakley, and T. Rakow. *Uncertain Judgements: Eliciting Expert Probabilities*. John Wiley, Chichester, 2006. URL <http://oro.open.ac.uk/17948/>.
- [88] Sarah Lichtenstein, Baruch Fischhoff, and Lawrence D Phillips. Calibration of probabilities: The state of the art. *Decision making and change in human affairs*, pages 275–324, 1977.
- [89] Amos Tversky and Daniel Kahneman. On the reality of cognitive illusions. *Psychological Review*, 103(3):582–591, 1996.
- [90] Michiel A Bakker, Duy Patrick Tu, Krishna P Gummadi, Alex Sandy Pentland, Kush R Varshney, and Adrian Weller. Beyond reasonable doubt: Improving fairness in budget-constrained decision making using confidence thresholds. In *Proceedings of the 2021 AAAI/ACM Conference on AI, Ethics, and Society*, pages 346–356, 2021.
- [91] Frank E Harrell, Robert M Califf, David B Pryor, Kerry L Lee, and Robert A Rosati. Evaluating the yield of medical tests. *Jama*, 247(18):2543–2546, 1982.
- [92] Eleftherios Mylonakis, Maria Paliou, Thomas C Greenbough, Timothy P Flanigan, Norman L Letvin, and Josiah D Rich. Report of a false-positive hiv test result and the potential use of additional tests in establishing hiv serostatus. *Archives of internal medicine*, 160(15):2386–2388, 2000.
- [93] Reiichiro Nakano, Jacob Hilton, Suchir Balaji, Jeff Wu, Long Ouyang, Christina Kim, Christopher Hesse, Shantanu Jain, Vineet Kosaraju, William Saunders, Xu Jiang, Karl Cobbe, Tyna Eloundou, Gretchen Krueger, Kevin Button, Matthew Knight, Benjamin Chess, and John Schulman. Webgpt: Browser-assisted question-answering with human feedback. *CoRR*, abs/2112.09332, 2021. URL <https://arxiv.org/abs/2112.09332>.
- [94] M Krishna Erramilli. Nationality and subsidiary ownership patterns in multinational corporations. *Journal of International Business Studies*, 27:225–248, 1996.
- [95] Kaisa Miettinen. Introduction to multiobjective optimization: Noninteractive approaches. In *Multiobjective optimization*, pages 1–26. Springer, 2008.

- [96] Natalia Martinez, Martin Bertran, and Guillermo Sapiro. Minimax pareto fairness: A multi objective perspective. In *International Conference on Machine Learning*, pages 6755–6764. PMLR, 2020.
- [97] Arthur M Geoffrion. Proper efficiency and the theory of vector maximization. *Journal of mathematical analysis and applications*, 22(3):618–630, 1968.
- [98] Shai Ben-David, John Blitzer, Koby Crammer, and Fernando Pereira. Analysis of representations for domain adaptation. *Advances in neural information processing systems*, 19, 2006.
- [99] Kaiming He, Xiangyu Zhang, Shaoqing Ren, and Jian Sun. Deep residual learning for image recognition. In *CVPR*, pages 770–778, 2016.
- [100] Ruairidh M Battleday, Joshua C Peterson, and Thomas L Griffiths. Capturing human categorization of natural images by combining deep networks and cognitive models. *Nature communications*, 11(1):1–14, 2020.

A Comparison Against Prior Work

Most papers on human-AI collaboration have considered clever ways of abstaining from prediction on specific inputs [44, 45], learning deferral functions based on multiple experts [46, 20], or teaching decision-makers when to rely [47]. There are also a number of papers from the HCI literature (see survey by [23]) that evaluate the two-action setting of our formulation using a *static* policy (e.g., always showing the ML model prediction or always showing some form of explanation).

To clarify how our set-up and assumptions differ from prior work, we overview work that we believe could be considered most similar to ours. We decompose our comparisons along a few dimensions: **Decision-support set-up:** Does the human make the final decision or is it a different set-up? **Assumptions about decision-maker information:** What does prior work assume about access to a decision-maker when learning a policy? **Evaluation:** Does prior work simulate humans? Does prior work run user studies?

Mozannar and Sontag [13]:

- **Decision-support set-up:** This work’s set-up can be considered a two-action setting of our formulation, where $\mathcal{A} = \{\text{DEFER}, \text{MODEL}\}$. Extending the work of Madras et al. [19], this work proposes the learning to defer paradigm, where the decision-maker may not always make a final decision (i.e., sometimes the decision is deferred entirely to an algorithmic-based system). In our set-up, deferring to a **MODEL** is equivalent to always adhering to a label-based form of support. The human is always the final decision-maker in our work, which is representative of many decision-making set-ups in practice [48], but not captured in this line of prior work.
- **Assumptions about decision-maker information:** This work assumes oracle query access to the decision-maker, for whom they are learning a policy.
- **Evaluation:** This work evaluates their approach using human simulations (no real human user studies).

Gao et al. [18] and Gao et al. [28]:

- **Decision-support set-up:** This work defines two actions: $\mathcal{A} = \{\text{DEFER}, \text{MODEL}\}$. They do not consider the, more practical assumption that the decision-maker will view a model prediction before making a decision themselves. Their formulation is similar to the above but they use offline bandits to learn a suitable policy.
- **Assumptions about decision-maker information:** Gao et al. [18] assume that understanding decision-maker’s expertise (at a population-level, not at a individual-level) can help learn better routing functions (i.e., defer only when appropriate). Gao et al. [28] assume access to a decision history for each decision-maker.
- **Evaluation:** They run a human subject experiment to collect offline annotations, which can be used to learn when to defer to decision-makers. Gao et al. [28] goes further to personalize a deferral policy based on offline annotations for each decision-maker.

Bordt and Von Luxburg [49]:

- **Decision-support set-up:** This work’s set-up can be considered a two-action setting of our formulation, where $\mathcal{A} = \{\text{DEFER}, \text{SHOW}\}$; however, they are concerned with the learnability of such a set up. They do not devise algorithms for this setting, as they are only focused on its theoretical formulation.
- **Assumptions about decision-maker information:** They assume the decision-maker has access to information not contained in the input but still important to the task.

- **Evaluation:** This is a theory paper, containing neither computational nor human subject experiments.

Noti and Chen [50]:

- **Decision-support set-up:** This work’s set-up can be considered as a two-action setting of our formulation, where $\mathcal{A} = \{\text{DEFER}, \text{SHOW}\}$. This is not an online algorithm and as such, the policy does not update.
- **Assumptions about decision-maker information:** They assume access to a dataset of human decisions and that all decision-makers are similar (i.e., they deploy one policy for all decision-makers).
- **Evaluation:** This work is one of few that runs a user study to evaluate their (fixed) policy on unseen decision-makers.

Babbar et al. [26]:

- **Decision-support set-up:** This work considers the two-action setting of our formulation, where $\mathcal{A} = \{\text{DEFER}, \text{CONFORMAL}\}$. Their policy is learned offline, is the same for all decision-makers, and is not updated in real-time based on decision-maker behavior.
- **Assumptions about decision-maker information:** They use CIFAR-10H [39] to learn a population-level deferral policy. This assumes that we have annotations for each decision-maker for every datapoint and assumes that all new decision-makers have the same competencies as the population average.
- **Evaluation:** This work runs a user study to evaluate their (fixed) policy. They show the benefits of DEFER+CONFORMAL over CONFORMAL or SHOW alone.

Wolczynski et al. [51]:

- **Decision-support set-up:** This work considers two actions per our formulation, where $\mathcal{A} = \{\text{DEFER}, \text{SHOW}\}$. They learn a rule-based policy offline, and deploy the same policy for all decision-makers.
- **Assumptions about decision-maker information:** They simulate human behavior by considering explicit functions of how human expertise may vary in input space.
- **Evaluation:** While this work does consider the human to be the final decision-maker, they only validate their proposal in simulation, not on actual human subjects.

We now list various forms of support that can be included in the action space of our problem formulation. The design of the action space is up to domain experts, who can decide not only which actions are feasible but also how much cost to assign to each form of support.

- **DEFER:** This form of support is equivalent to **no support**. Decision-makers are asked to make a decision without any assistance. The machine learning community has studied how to identify when to defer to a subset of examples to humans based on human strengths [52, 53] and/or model failures [54, 55]. The premise of such an action would be to allow human decision-makers to be unaided and squarely placing decision liability on the individual.
- **SHOW:** In many settings, machine learning (ML) models are trained to do prediction tasks similar to the decision-making task prescribed to the human, or in the case of foundation models [5], ML systems can be adapted to aid decision-making, even if the task was not specifically prescribed at train-time [56]. In essence, a machine learning model prediction, or associated generation (e.g., a code snippet [57]) would be shown to aid an individual decision-maker. This has been shown to help improve decision-maker performance. The following are variations of showing a model prediction to a decision-maker.

- **CONFORMAL**: For classification tasks, only displaying the most likely label may not lead to good performance due to various reasons, including uncertainty in the modeling procedure [58, 59]; however, such uncertainty can be communicated to decision-maker by showing a prediction set to experts [26]. Such a prediction set might be generated using conformal prediction, which guarantees the true label lies in the set with a user-specified error tolerance [60, 61].
- **CONFIDENCE**: Instead of translating the uncertainty into a prediction set (or interval), one could simply show the confidence or uncertainty of the prediction, which may manifest as displaying probabilities, standard errors, or entropies [62, 63]. The visualization mechanism used for displaying confidence may alter the decision-maker’s performance [64, 25].
- **EXPLAIN**: In addition to providing a model prediction, many have considered showing an explanation of model behavior, examples of which include feature attribution [65, 66], sample importance [67, 68], counterfactual explanations [69, 70], and natural language rationales [71, 72]. Displaying such explanations to end users has had mixed results on how decision-making performance is affected [73, 48]. Worryingly, in many settings, showing some types of explanations may lead to over-reliance on models by giving the perception of competence [66, 74, 75].
- **CONSENSUS**: One can also depict forms of support that are independent of any model, for instance, presenting the belief of one or more humans. Belief distributions can be constructed by pooling over many different humans’ “votes” for what a label ought to be, e.g., [39, 76, 77, 78, 79, 80], or by eliciting distributions over the likely label directly from each individual human [81, 82]. These consensus distributions permit the expression of uncertainty *without any model*. However, the elicitation of this form of support may be costly and humans may be fallible in the information they provide, e.g., due to direct labeling errors [83, 84, 85, 86], or miscalibrated confidence [87, 82, 88, 89].
- **ADDITIONAL**: While much of this paper focused on support that provides decision-makers with label information, decision support may also entail acquiring or displaying additional contextual information (e.g., new features [90]) or requesting previously unseen features, for instance, through additional medical diagnostics [91, 92]. This flavor of support can be varied structurally, ranging from the results of a search query [93] to hierarchical information like exposing the subsidiary ownership structure for multinational corporations [94]. In terms of the costs incurred, some pieces of additional information may require additional cost, or certification if pertaining to sensitive attributes.

B Additional Details on Problem Formulation

B.1 Pareto Optimality

We use dominance [95] to define Pareto optimality for the MOO problem in Eq. 3.

Definition B.1 (Dominant policy). A policy π is said to dominate another policy π' , noted as $\pi \prec \pi'$, if the following holds: (i) $r_h(\pi) \leq r_h(\pi')$ and $c(\pi) \leq c(\pi')$; and (ii) either $r_h(\pi) < r_h(\pi')$ or $c(\pi) < c(\pi')$. Likewise, we denote $\pi \preceq \pi'$ if $\pi' \not\prec \pi$.

Definition B.2 (Pareto front and Pareto optimality). Given a set of policies Π , the set of Pareto front policies is $\mathcal{P}_\Pi = \{\pi \in \Pi : \nexists \pi' \in \Pi \text{ s.t. } \pi' \prec \pi\}$. The corresponding Pareto front is given by $\mathcal{P}_\Pi^{\mathcal{R}_h} = \{(v_1, v_2) \in \mathbb{R}^2 : \exists \pi \in \mathcal{P}_\Pi \text{ s.t. } v_1 = r_h(\pi) \text{ and } v_2 = c(\pi)\}$. A policy π is a Pareto optimal solution to the MOO problem in Eq. 3 iff $\pi \in \mathcal{P}_\Pi$.

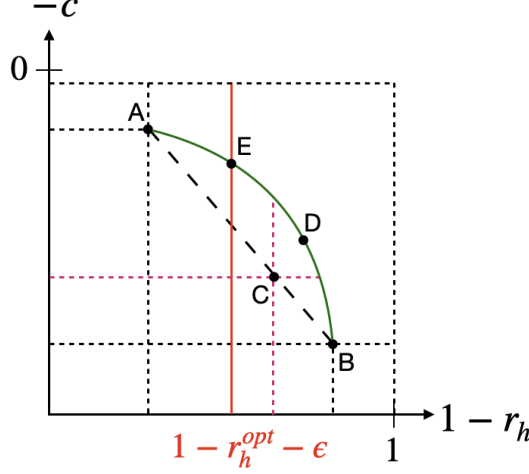


Figure 6: The green curve corresponds to the (unknown) Pareto front of the MOO problem in Eq. 3, e.g., $A = (1 - r_h(\pi_0^*), -c(\pi_0^*))$, $B = (1 - r_h(\pi_1^*), -c(\pi_1^*))$, and $D = (1 - r_h(\pi_\lambda^*), -c(\pi_\lambda^*))$ for some $\lambda \in (0, 1)$. The point $E = (1 - r_h(\pi^\epsilon), -c(\pi^\epsilon))$ corresponds to the constrained optimisation problem Eq. 6, which is the point on the curve that we would like our decision support policy to achieve. The dashed line corresponds to the set $\{\pi_\mu := \mu \cdot \pi_0^* + (1 - \mu) \cdot \pi_1^* : \mu \in [0, 1]\}$, e.g., $C = (1 - r_h(\pi_\mu), -c(\pi_\mu))$ for some $\mu \in (0, 1)$. While the set of Pareto optimal policies Π_h^{opt} may be difficult to compute without further assumptions, we propose a tractable proxy $\{\pi_\mu\}$, that can be recovered if one is able to compute π_0^* and π_1^* , which would already require accurate estimation of $r_h(x, a)$ values for all x and a .

Definition B.3 (Convex Pareto front). A Pareto front $\mathcal{P}_\Pi^{\mathcal{R}_h}$ is convex if $\forall v, v' \in \mathcal{P}_\Pi^{\mathcal{R}_h}, \lambda \in [0, 1]$, $\exists v_\lambda \in \mathcal{P}_\Pi^{\mathcal{R}_h}$ such that $v_\lambda \preceq \lambda \cdot v + (1 - \lambda) \cdot v'$.

Note that optimal solutions to the SOO problem in Eq. 4 are Pareto optimal solutions to the MOO problem in Eq. 3. In the following proposition, we show that the Pareto front $\mathcal{P}_\Pi^{\mathcal{R}_h}$ of the MOO problem in Eq. 3 can be fully characterized by the solutions of the SOO problem in Eq. 4, i.e., any Pareto optimal policy $\pi \in \mathcal{P}_\Pi$ is a solution to the SOO problem in Eq. 4 for some choice of $\lambda \in [0, 1]$.

Proposition B.4. *The Pareto front of the MOO problem in Eq. 3 is convex:*

$\forall v, v' \in \mathcal{P}_\Pi^{\mathcal{R}_h}, \lambda \in [0, 1], \exists v'' \in \mathcal{P}_\Pi^{\mathcal{R}_h} : v'' \preceq \lambda \cdot v + (1 - \lambda) \cdot v'$. Every Pareto solution of the MOO problem in Eq. 3 is a solution to the SOO problem in Eq. 4: $\forall v \in \mathcal{P}_\Pi^{\mathcal{R}_h}, \exists \lambda : v = [r_h(\pi_\lambda^*), c(\pi_\lambda^*)]^\top$.

Proof. First, we note that the set of stochastic policies Π is a convex set, and both $r_h : \Pi \rightarrow [0, 1]$ and $c : \Pi \rightarrow [0, 1]$ are convex functions. Then, the first statement of the proposition follows from Theorem 4.1 of [96]. The second statement is a direct application of the results in [97]. \square

B.2 Reframing the Objective

Here, we show that the solution to the SOO problem in Eq. 4 can be written as Eq. 5. Consider the following:

$$\begin{aligned}
 \pi_\lambda^* &= \arg \min_{\pi \in \Pi} \lambda \cdot r_h(\pi) + (1 - \lambda) \cdot c(\pi) \\
 &= \arg \min_{\pi \in \Pi} \lambda \cdot \mathbb{E}_x \left[\sum_{i=1}^k \pi(x)_{A_i} \cdot \mathbb{E}_{y|x} [\ell(y, h(x, A_i))] \right] + (1 - \lambda) \cdot \mathbb{E}_x \left[\sum_{i=1}^k \pi(x)_{A_i} \cdot c(A_i) \right] \\
 &= \arg \min_{\pi \in \Pi} \sum_{i=1}^k \pi(x)_{A_i} \cdot \mathbb{E}_x [\lambda \cdot \mathbb{E}_{y|x} [\ell(y, h(x, A_i))] + (1 - \lambda) \cdot c(A_i)]
 \end{aligned}$$

$$= \arg \min_{\pi \in \Pi} \sum_{i=1}^k \pi(x)_{A_i} \cdot \mathbb{E}_x [\lambda \cdot r_{A_i}(x; h) + (1 - \lambda) \cdot c(A_i)],$$

where the objective in the last step is minimized by the solution in Eq. 5.

B.3 Misspecification

We upper bound the misspecification error of applying a policy π_h (originally learned for human h) on human \tilde{h} . Inspired by [98], we define $\Pi\Delta\Pi$ -divergence to bound the human misspecification error. Let $L_h(\pi, \pi') = \mathbb{E}_x[\ell(h(x, \pi(x)), h(x, \pi'(x)))]$ be the expected disagreement between two policies π and π' for human h . The $\Pi\Delta\Pi$ -divergence between two humans h and \tilde{h} is defined as $d_{\Pi\Delta\Pi}(h, \tilde{h}) = \sup_{\pi, \pi' \in \Pi} |L_h(\pi, \pi') - L_{\tilde{h}}(\pi, \pi')|$. Based on this divergence measure, we bound the risk $r_{\tilde{h}}(\pi_h) = \mathbb{E}_{(x,y) \sim \mathcal{P}}[\ell(y, \tilde{h}(x, \pi_h(x)))]$ of using policy π_h on human \tilde{h} as follows:

$$r_{\tilde{h}}(\pi_h) \leq r_h(\pi_h) + d_{\Pi\Delta\Pi}(h, \tilde{h}) + \lambda_{\Pi},$$

where $\lambda_{\Pi} = \inf_{\pi' \in \Pi} [r_h(\pi') + r_{\tilde{h}}(\pi')]$.

B.4 Measuring overall performance

Ideally, we evaluate the overall performance of the sequence of policies $\{\pi_t\}_{t=1}^T$ learned by **Modiste** using the following:

$$\text{Overall Performance}(\text{Modiste}) = \text{Bias}(\text{SELECT}) + \text{Regret}(\text{THREAD})$$

$$\begin{aligned} \frac{1}{T} \sum_t r_{h_{\text{real}}}(\pi_t) - r_{h_{\text{real}}}(\pi^{\epsilon, \text{real}}) &= \left[r_{h_{\text{real}}}(\pi_{\lambda_{\text{sim}}}^{*, \text{real}}) - r_{h_{\text{real}}}(\pi^{\epsilon, \text{real}}) \right] + \frac{1}{T} \sum_t r_{h_{\text{real}}}(\pi_t) - r_{h_{\text{real}}}(\pi_{\lambda_{\text{sim}}}^{*, \text{real}}) \\ \frac{1}{T} \sum_t c(\pi_t) - c(\pi^{\epsilon, \text{real}}) &= \left[c(\pi_{\lambda_{\text{sim}}}^{*, \text{real}}) - c(\pi^{\epsilon, \text{real}}) \right] + \frac{1}{T} \sum_t c(\pi_t) - c(\pi_{\lambda_{\text{sim}}}^{*, \text{real}}) \end{aligned}$$

However, this proves to be challenging. Specifically, we have access to neither $\pi_{\lambda_{\text{sim}}}^{*, \text{real}}$ nor $\pi^{\epsilon, \text{real}}$. This makes it impossible to compute either term in practice. Thus, we resort to using expected loss (Eq. 1) and cost (Eq. 2) to validate our methods.

B.5 Algorithms

We present specific implementations of **THREAD** (Algorithm 1) using LinUCB and online KNN in Algorithm 2 and 3, respectively.

Algorithm 2 THREAD using LinUCB

- 1: **Input:** trade-off parameter λ ; human decision-maker h ; cost function $c : \mathcal{A} \rightarrow [0, 1]$; UCB parameter α
- 2: **Initialization:** data buffer $\mathcal{D}_0 = \{\}$; $\mathbf{A}_a = \mathbf{I}_{p \times p}$ and $\mathbf{b}_a = \mathbf{0}_{p \times 1}$ for all $a \in \mathcal{A}$; $\{\theta_a = (\mathbf{A}_a)^{-1} \mathbf{b}_a : a \in \mathcal{A}\}$; human prediction error values $\{\hat{r}_{a,0}(x; h) = \langle \theta_a, x \rangle : x \in \mathcal{X}, a \in \mathcal{A}\}$; initial policy $\pi_1(x)_a = 1/|\mathcal{A}|$ for all $a \in \mathcal{A}$
- 3: **for** $t = 1, 2, \dots, T$ **do**
- 4: data point $(x_t, y_t) \in \mathcal{X} \times \mathcal{Y}$ is drawn iid from \mathcal{P} (normalized s.t. $\|x_t\|_2 \leq 1$)
- 5: support $a_t \in \mathcal{A}$ is selected using policy π_t
- 6: human makes the prediction \tilde{y}_t based on x_t and a_t
- 7: human incurs the loss $\ell(y_t, \tilde{y}_t)$
- 8: update the buffer $\mathcal{D}_t \leftarrow \mathcal{D}_{t-1} \cup \{(x_t, a_t, \ell(y_t, \tilde{y}_t))\}$
- 9: update the decision support policy:

$$\begin{aligned}
 \mathbf{A}_{a_t} &\leftarrow \mathbf{A}_{a_t} + x_t x_t^\top \\
 \mathbf{b}_{a_t} &\leftarrow \mathbf{b}_{a_t} + r_t x_t \\
 \theta_a &\leftarrow (\mathbf{A}_a)^{-1} \mathbf{b}_a \text{ for all } a \in \mathcal{A} \\
 \hat{r}_{a,t}(x; h) &\leftarrow \langle \theta_a, x \rangle \text{ for all } a \in \mathcal{A} & \text{(Step 1)} \\
 \pi_{t+1}(x) &\leftarrow \arg \min_{a \in \mathcal{A}} \lambda \cdot \hat{r}_{a,t}(x; h) + (1 - \lambda) \cdot c(a) - \alpha \cdot \sqrt{x^\top (\mathbf{A}_a)^{-1} x} & \text{(Step 2)}
 \end{aligned}$$

10: **end for**

11: **Output:** policy $\pi_\lambda^{\text{alg}} \leftarrow \pi_{T+1}$

Algorithm 3 THREAD using online KNN

- 1: **Input:** trade-off parameter λ ; human decision-maker h ; cost function $c : \mathcal{A} \rightarrow [0, 1]$; warm-up steps W ; number of neighbours K ; exploration parameter γ
- 2: **Initialization:** data buffer $\mathcal{D}_0 = \{\}$; human prediction error values $\{\hat{r}_{a,0}(x; h) = 0.5 : x \in \mathcal{X}, a \in \mathcal{A}\}$; initial policy $\pi_1(x)_a = 1/|\mathcal{A}|$ for all $a \in \mathcal{A}$
- 3: **for** $t = 1, 2, \dots, T$ **do**
- 4: data point $(x_t, y_t) \in \mathcal{X} \times \mathcal{Y}$ is drawn iid from \mathcal{P}
- 5: support $a_t \in \mathcal{A}$ is selected using policy π_t
- 6: human makes the prediction \tilde{y}_t based on x_t and a_t
- 7: human incurs the loss $\ell(y_t, \tilde{y}_t)$
- 8: update the buffer $\mathcal{D}_t \leftarrow \mathcal{D}_{t-1} \cup \{(x_t, a_t, \ell(y_t, \tilde{y}_t))\}$
- 9: update the decision support policy:

$$\begin{aligned}
\mathcal{N}(x) &\leftarrow K \text{ neighbouring data points for } x \text{ in } \mathcal{D}_t \\
\mathcal{N}_a(x) &\leftarrow \{(x_i, a_i, \ell(y_i, \tilde{y}_i)) : (x_i, a_i, \ell(y_i, \tilde{y}_i)) \in \mathcal{N}(x) \text{ and } a_i = a\} \quad \text{for all } a \in \mathcal{A} \\
\hat{r}_{a,t}(x; h) &\leftarrow \frac{1}{|\mathcal{N}_a(x)|} \cdot \sum_{(x_i, a_i, \ell(y_i, \tilde{y}_i)) \in \mathcal{N}_a(x)} \ell(y_i, \tilde{y}_i) \quad \text{for all } a \in \mathcal{A} \text{ with } |\mathcal{N}_a(x)| > 0
\end{aligned}
\tag{Step 1}$$

$$\begin{aligned}
\pi_{\text{rand}}(x)_a &\leftarrow \frac{1}{|\mathcal{A}|} \quad \text{for all } a \in \mathcal{A} \\
\pi_{\text{knn}}(x) &\leftarrow \arg \min_{a \in \mathcal{A}} \lambda \cdot \hat{r}_{a,t}(x; h) + (1 - \lambda) \cdot c(a) \\
\pi_{t+1}(x) &\leftarrow \pi_{\text{rand}}(x) \quad \text{if } t \leq W \tag{Step 2} \\
\pi_{t+1}(x) &\leftarrow \gamma \cdot \pi_{\text{rand}}(x) + (1 - \gamma) \cdot \pi_{\text{knn}}(x) \quad \text{if } t > W \tag{Step 2}
\end{aligned}$$

10: **end for**

11: **Output:** policy $\pi_\lambda^{\text{alg}} \leftarrow \pi_{T+1}$

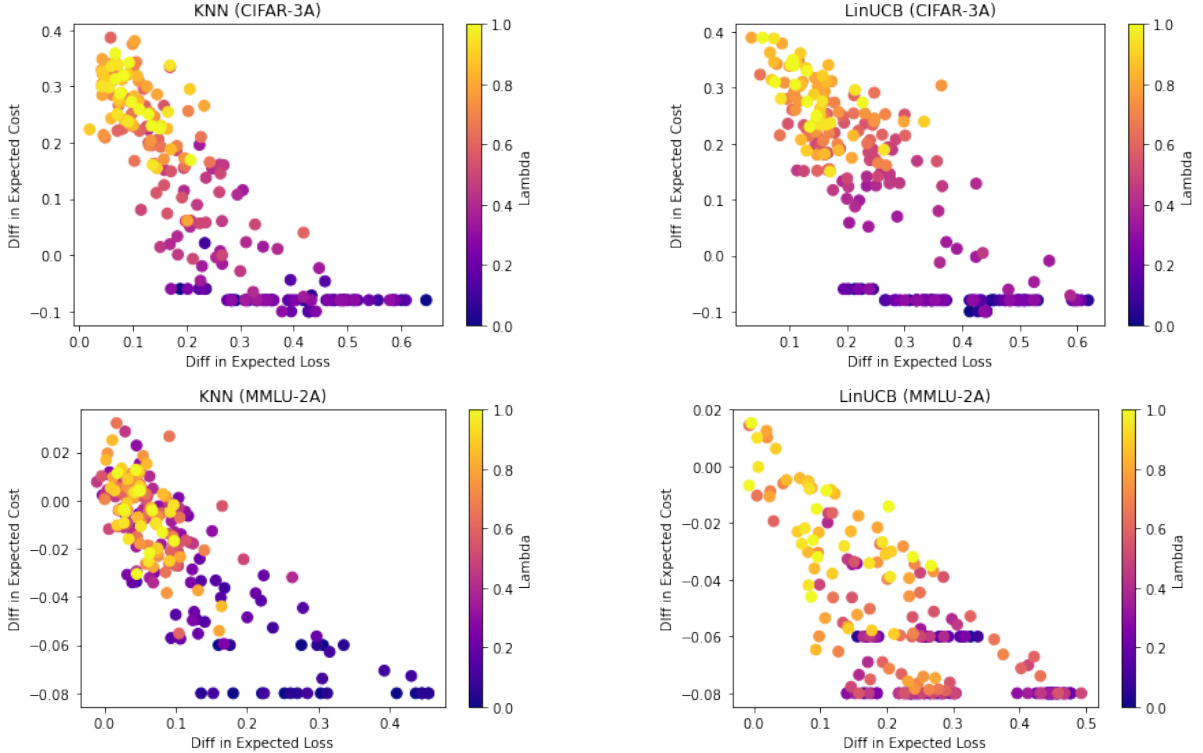


Figure 7: Top is CIFAR-3A and Bottom is MMLU-2A. For each of the $N = 10$ simulators, we instantiate using the population data, we compute the difference in expected loss between the optimal policy for that simulator and the learned policy for all values of $\lambda \in [0, 1]$ in increments of 0.05, and compute the difference in expected cost in the same manner. For KNN, we observe overlap between many values of λ that all come within ϵ of the Best Risk: this implies we can use lower values of λ to potentially achieve the desired level of performance. For LinUCB, we find that large values of λ are required to achieve a suitable level of performance.

C Additional Computational Experiments and Details

C.1 Dataset Details

C.1.1 CIFAR

To explore the performance of our algorithms in both separable and non-separable settings, we construct two subvariants of the CIFAR-10 [35] image dataset. As depicted in Figure 8, we subsample from the CIFAR embeddings to create linearly separable classes. Embeddings are constructed by running t-SNE on the 512-dimensional latent codes extracted by the penultimate layer of a variant of the VGG architecture (VGG-11) [99] trained on the animal class subset of CIFAR; the model attained an accuracy of 89.5%. We filter the original 10 CIFAR classes to only include those involving animals (Birds, Cats, Deers, Dogs, Frogs, and Horses). We consider at most 5 such classes in our experiments (dropping Dog).

C.1.2 MMLU

We consider questions from four topics of MMLU (elementary mathematics, high school biology, high school computer science, and US foreign policy). Topic names match those proposed in [36]. We select topics to cover span an array of disciplines across the sciences and humanities, as discussed in Appendix D. We use questions in the MMLU test set for each topic that are at most 150 characters long. We limit the length of questions to facilitate readability in our human user studies and wanted to maximize parity between our computational and human experiments by considering the same set of questions across both set-ups. This yields 264, 197, 98, and 47 questions for the elementary mathematics, high school biology, US foreign policy, and high school computer science topics, respectively. We emphasize that in CIFAR, our arms operate in label space – in contrast, with MMLU, arm selection is in *covariate* (topic) space – further highlighting the flexibility of our adaptive support paradigm.

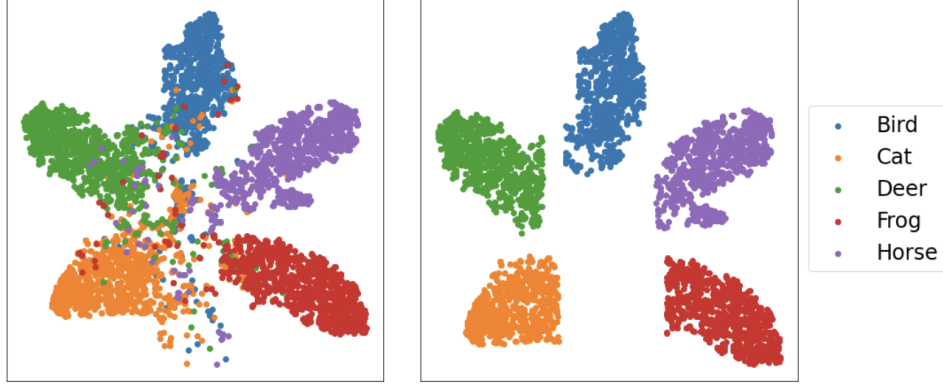


Figure 8: We depict the latent space of the CIFAR subset used. Embeddings without filtering (left) and after filtering out points that violate separability of classes (right). We use the embeddings on the right for our Synthetic-2A task and the left for the natural CIFAR tasks.

We leverage OpenAI’s LLM-based embedding model (`text-embedding-ada-003`), to produce embeddings over the question prompts. Embedding vectors extracted via OpenAI’s API are by default length 1536; we apply t-SNE, like in the CIFAR tasks, to compress the embeddings into two-dimensional latent codes per example. Nicely, these latents are already separable (see Figure 5; no post-filtering is applied to ensure separability).

C.2 Additional Computational Experiments

Table 2: Unlike Table 1 where risks come from pilot studies, we instantiate simulated **synthetic** humans, each specified by the human’s loss on each form of support H-ONLY (Human only) and H-MODEL (Human+Model), for MMLU-2A. We report the expected loss $r_h(\pi)$ and the expected cost $c(\pi)$ —for both metrics, lower is better—averaged across the last 10 steps of 100 total time steps along with their standard deviations (across 5 runs). We bold the algorithm that achieves the lowest cost within ϵ of the Best Risk for each human simulation and find that our algorithm outperforms baselines on various simulated humans. For each form of support, we specify risk r over each of the 4 topics for MMLU-2A. We fix the cost structure: $c(\text{H-ONLY}) = 0.0$ and $c(\text{H-MODEL}) = 0.1$. The selected λ values used for THREAD are in Table 3. For THREAD, we select the best policy over a sweep of λ values that minimizes Eq. 6 under $\epsilon = 0.05$. We also indicate the values of λ chosen beneath the results table.

| Algorithm | | $r_{A_1} = [0.8, 0.8, 0.1, 0.1]$ $r_{A_2} = [0.2, 0.1, 0.1, 0.2]$ | | $r_{A_1} = [0.2, 0.8, 0.1, 0.1]$ $r_{A_2} = [0.8, 0.1, 0.1, 0.2]$ | | $r_{A_1} = [0.2, 0.5, 0.5, 0.8]$ $r_{A_2} = [0.8, 0.1, 0.1, 0.8]$ | |
|-----------|-----------------------------------|--|-----------------------------------|--|-----------------------------------|--|-----------------------------------|
| | | $r_h(\pi)$ | $c(\pi)$ | $r_h(\pi)$ | $c(\pi)$ | $r_h(\pi)$ | $c(\pi)$ |
| MMLU-2A | H-ONLY ($\pi_{\lambda=0}^*$) | 0.45 ± 0.04 | 0.0 | 0.33 ± 0.06 | 0.0 | 0.51 ± 0.04 | 0.0 |
| | H-MODEL | 0.14 ± 0.02 | 0.1 | 0.30 ± 0.05 | 0.1 | 0.45 ± 0.04 | 0.1 |
| | Human Pop | 0.45 ± 0.07 | 0.05 ± 0.01 | 0.22 ± 0.08 | 0.06 ± 0.01 | 0.41 ± 0.04 | 0.05 ± 0.01 |
| | THREAD-LinUCB | 0.15 ± 0.04 | 0.05 ± 0.06 | 0.19 ± 0.07 | 0.05 ± 0.02 | 0.39 ± 0.08 | 0.06 ± 0.01 |
| | THREAD-KNN | 0.14 ± 0.06 | 0.04 ± 0.01 | 0.13 ± 0.04 | 0.03 ± 0.04 | 0.33 ± 0.05 | 0.05 ± 0.01 |
| | Best Risk ($\pi_{\lambda=1}^*$) | 0.13 | 0.05 | 0.13 | 0.03 | 0.3 | 0.05 |

| Algorithm | | $r_{A_1} = [0.8, 0.8, 0.1, 0.1]$ $r_{A_2} = [0.2, 0.1, 0.1, 0.2]$ | $r_{A_1} = [0.2, 0.8, 0.1, 0.1]$ $r_{A_2} = [0.8, 0.1, 0.1, 0.2]$ | $r_{A_1} = [0.2, 0.5, 0.5, 0.8]$ $r_{A_2} = [0.8, 0.1, 0.1, 0.8]$ |
|-----------|---------------|--|--|--|
| | | | | |
| MMLU-2A | THREAD-LinUCB | 1.0 | 0.9 | 1.0 |
| | THREAD-KNN | 0.3 | 0.2 | 0.3 |

In Table 2, we provide additional computational results for CIFAR-2A and MMLU-2A. We find that THREAD successfully personalizes decision support policies that trade-off cost and performance effectively. We note that in all of our experiments, we fix the exploration parameters in LinUCB and KNN (i.e., $\alpha = 1$ and $\gamma = 0.1$ respectively). However, we do explore varying these exploration parameters in Table 4.

Varying KNN Parameters. While LinUCB does not require identifying additional parameters, KNN has two: K which is the number of nearest neighbors to select when estimating the risk of a form

Table 3: The best value of λ that is selected from doing a sweep over $\lambda \in [0, 1]$ that corresponds to the human simulators in Table 1.

| Algorithm | | $r_{A_1} = [0.7, 0.1, 0.7]$ $r_{A_2} = [0.1, 0.1, 0.1]$ | $r_{A_1} = [0.7, 0.1, 0.7]$ $r_{A_2} = [0.1, 0.7, 0.1]$ | $r_{A_1} = [0.7, 0.1, 0.7]$ $r_{A_2} = [0.7, 0.7, 0.1]$ |
|--------------|---------------|--|--|--|
| Synthetic-2A | THREAD-LinUCB | 0.4 | 0.6 | 0.6 |
| | THREAD-KNN | 0.9 | 0.6 | 0.6 |
| CIFAR-2A | THREAD-LinUCB | 0.4 | 0.9 | 0.5 |
| | THREAD-KNN | 0.7 | 0.9 | 0.6 |

| Algorithm | | Best alone | Lowest Best Risk | Highest Best Risk |
|-----------|---------------|------------|------------------|-------------------|
| CIFAR-3A | THREAD-LinUCB | 0.85 | 0.8 | 0.9 |
| | THREAD-KNN | 1.0 | 0.9 | 0.9 |
| MMLU-2A | THREAD-LinUCB | 0.7 | 0.95 | 1.0 |
| | THREAD-KNN | 0.25 | 0.6 | 0.35 |

Table 4: Vary exploration parameters (α for LinUCB and γ for KNN). We find that LinUCB generally performs better when exploration increases and KNN generally performs better when exploration decreases.

| Algorithm | | $r_{A_1} = [0.7, 0.1, 0.7]$ $r_{A_2} = [0.1, 0.1, 0.1]$ | | $r_{A_1} = [0.7, 0.1, 0.7]$ $r_{A_2} = [0.1, 0.7, 0.1]$ | | $r_{A_1} = [0.7, 0.1, 0.7]$ $r_{A_2} = [0.7, 0.7, 0.1]$ | |
|--------------|----------------------------------|--|-----------------|--|-----------------|--|-----------------|
| | | $r_h(\pi)$ | $c(\pi)$ | $r_h(\pi)$ | $c(\pi)$ | $r_h(\pi)$ | $c(\pi)$ |
| Synthetic-2A | THREAD-LinUCB ($\alpha = 0.1$) | 0.14 ± 0.04 | 0.33 ± 0.02 | 0.19 ± 0.09 | 0.32 ± 0.02 | 0.34 ± 0.10 | 0.21 ± 0.07 |
| | THREAD-LinUCB ($\alpha = 10$) | 0.13 ± 0.04 | 0.32 ± 0.03 | 0.12 ± 0.03 | 0.33 ± 0.02 | 0.30 ± 0.05 | 0.23 ± 0.07 |
| | THREAD-KNN ($\gamma = 0.01$) | 0.12 ± 0.04 | 0.35 ± 0.06 | 0.19 ± 0.08 | 0.26 ± 0.07 | 0.33 ± 0.04 | 0.20 ± 0.03 |
| | THREAD-KNN ($\gamma = 0.2$) | 0.16 ± 0.05 | 0.33 ± 0.04 | 0.21 ± 0.06 | 0.24 ± 0.03 | 0.34 ± 0.06 | 0.15 ± 0.02 |
| CIFAR-2A | THREAD-LinUCB ($\alpha = 0.1$) | 0.15 ± 0.08 | 0.30 ± 0.04 | 0.14 ± 0.05 | 0.32 ± 0.02 | 0.31 ± 0.05 | 0.26 ± 0.07 |
| | THREAD-LinUCB ($\alpha = 10$) | 0.14 ± 0.04 | 0.32 ± 0.02 | 0.18 ± 0.04 | 0.31 ± 0.02 | 0.32 ± 0.05 | 0.26 ± 0.08 |
| | THREAD-KNN ($\gamma = 0.01$) | 0.12 ± 0.03 | 0.33 ± 0.02 | 0.14 ± 0.06 | 0.31 ± 0.03 | 0.35 ± 0.06 | 0.14 ± 0.03 |
| | THREAD-KNN ($\gamma = 0.2$) | 0.17 ± 0.05 | 0.32 ± 0.06 | 0.20 ± 0.09 | 0.31 ± 0.03 | 0.35 ± 0.06 | 0.16 ± 0.04 |

| Algorithm | | $r_{A_1} = [0.8, 0.8, 0.1, 0.1]$ $r_{A_2} = [0.2, 0.1, 0.1, 0.2]$ | | $r_{A_1} = [0.2, 0.8, 0.1, 0.1]$ $r_{A_2} = [0.8, 0.1, 0.1, 0.2]$ | | $r_{A_1} = [0.2, 0.5, 0.5, 0.8]$ $r_{A_2} = [0.8, 0.1, 0.1, 0.8]$ | |
|-----------|----------------------------------|--|-----------------|--|-----------------|--|-----------------|
| | | $r_h(\pi)$ | $c(\pi)$ | $r_h(\pi)$ | $c(\pi)$ | $r_h(\pi)$ | $c(\pi)$ |
| MMLU-2A | THREAD-LinUCB ($\alpha = 0.1$) | 0.26 ± 0.06 | 0.03 ± 0.01 | 0.22 ± 0.09 | 0.04 ± 0.01 | 0.47 ± 0.08 | 0.03 ± 0.02 |
| | THREAD-LinUCB ($\alpha = 10$) | 0.15 ± 0.05 | 0.04 ± 0.01 | 0.18 ± 0.07 | 0.03 ± 0.01 | 0.40 ± 0.06 | 0.05 ± 0.01 |
| | THREAD-KNN ($\gamma = 0.01$) | 0.16 ± 0.05 | 0.05 ± 0.00 | 0.15 ± 0.06 | 0.03 ± 0.01 | 0.39 ± 0.06 | 0.03 ± 0.01 |
| | THREAD-KNN ($\gamma = 0.2$) | 0.15 ± 0.03 | 0.05 ± 0.01 | 0.12 ± 0.03 | 0.03 ± 0.00 | 0.38 ± 0.05 | 0.03 ± 0.01 |

of support and W which is the length of the warm-up period. In Table 5, we show that as long as K is reasonably sized (i.e. $K > 3$), the performance of KNN does not vary too much across datasets.

Table 5: We vary the K and W parameters used to instantiate KNN across three datasets and report the expected risk $r_h(\pi)$ (lower is better) and expected cost $c(\pi)$ (lower is better) across 5 runs. The human simulation used here is the same as the one used in the second setting of Table 2.

| | $K = 3, W = 10$ | | $K = 5, W = 10$ | | $K = 5, W = 25$ | | $K = 8, W = 40$ | |
|--------------|-----------------|-----------------|-----------------|-----------------|-----------------|-----------------|-----------------|-----------------|
| | $r_h(\pi)$ | $c(\pi)$ | $r_h(\pi)$ | $c(\pi)$ | $r_h(\pi)$ | $c(\pi)$ | $r_h(\pi)$ | $c(\pi)$ |
| Synthetic-2A | 0.20 ± 0.11 | 0.25 ± 0.08 | 0.15 ± 0.05 | 0.30 ± 0.03 | 0.14 ± 0.05 | 0.31 ± 0.03 | 0.12 ± 0.04 | 0.00 ± 0.00 |
| CIFAR-2A | 0.25 ± 0.15 | 0.24 ± 0.12 | 0.14 ± 0.04 | 0.34 ± 0.03 | 0.17 ± 0.04 | 0.30 ± 0.04 | 0.14 ± 0.04 | 0.32 ± 0.03 |
| MMLU-2A | 0.18 ± 0.07 | 0.03 ± 0.01 | 0.14 ± 0.04 | 0.03 ± 0.01 | 0.15 ± 0.03 | 0.04 ± 0.01 | 0.15 ± 0.04 | 0.03 ± 0.01 |

Varying Embedding Size. In the main text, we run computational experiments using a two-dimension t-SNE embedding. In Table 6 for CIFAR-2A, we consider how THREAD would behave when we vary dimensionality of \mathcal{X} . We extract higher dimensional embeddings from animal-class trained VGGs (see above) with varied penultimate layer widths, where width matches embedding size. While we opt for t-SNE embeddings, in the main paper, to provide a clearer visualizations, we find that strong performance holds even for high-dimensional embeddings. We expect that even larger embedding dimensions will permit THREAD to work in a variety of real-world contexts.

Multiple Arms Experiment. In Figure 9, we consider a setting of learning a policy with three forms of support: $\mathcal{A} = \{A_1, A_2, A_3\}$. Let $c(A_1) < c(A_2) = c(A_3)$. This is an analogous setup to what we

Table 6: On the CIFAR-2A dataset, we explore the effect of varying the embedding size for KNN, with $K = 8$, $W = 25$ (Top), and LinUCB (Bottom). We report the expected risk $r_h(\pi)$ (lower is better) and expected cost $c(\pi)$ (lower is better) averaged over 5 runs. Recall that in our experiments we used two-dimensional t-SNE embeddings, not model embeddings.

| Embedding Size | $r_{A_1} = [0.7, 0.1, 0.7]$ $r_{A_2} = [0.1, 0.7, 0.1]$ | | | | $r_{A_1} = [0.7, 0.1, 0.7]$ $r_{A_2} = [0.7, 0.7, 0.1]$ | | | |
|----------------|--|-----------------|-----------------|-----------------|--|-----------------|-----------------|-----------------|
| | $T = 100$ | | $T = 200$ | | $T = 100$ | | $T = 200$ | |
| | $r_h(\pi)$ | $c(\pi)$ | $r_h(\pi)$ | $c(\pi)$ | $r_h(\pi)$ | $c(\pi)$ | $r_h(\pi)$ | $c(\pi)$ |
| 2 | 0.18 ± 0.08 | 0.28 ± 0.06 | 0.14 ± 0.04 | 0.32 ± 0.03 | 0.32 ± 0.05 | 0.24 ± 0.06 | 0.33 ± 0.06 | 0.23 ± 0.05 |
| 4 | 0.18 ± 0.04 | 0.29 ± 0.04 | 0.16 ± 0.04 | 0.32 ± 0.03 | 0.33 ± 0.05 | 0.20 ± 0.05 | 0.33 ± 0.05 | 0.21 ± 0.04 |
| 8 | 0.15 ± 0.05 | 0.30 ± 0.04 | 0.15 ± 0.03 | 0.33 ± 0.03 | 0.32 ± 0.05 | 0.24 ± 0.04 | 0.33 ± 0.05 | 0.24 ± 0.06 |

| Embedding Size | $r_{A_1} = [0.7, 0.1, 0.7]$ $r_{A_2} = [0.1, 0.7, 0.1]$ | | | | $r_{A_1} = [0.7, 0.1, 0.7]$ $r_{A_2} = [0.7, 0.7, 0.1]$ | | | |
|----------------|--|-----------------|-----------------|-----------------|--|-----------------|-----------------|-----------------|
| | $T = 100$ | | $T = 200$ | | $T = 100$ | | $T = 200$ | |
| | $r_h(\pi)$ | $c(\pi)$ | $r_h(\pi)$ | $c(\pi)$ | $r_h(\pi)$ | $c(\pi)$ | $r_h(\pi)$ | $c(\pi)$ |
| 2 | 0.31 ± 0.05 | 0.19 ± 0.03 | 0.32 ± 0.04 | 0.20 ± 0.02 | 0.49 ± 0.05 | 0.10 ± 0.08 | 0.49 ± 0.05 | 0.11 ± 0.08 |
| 4 | 0.14 ± 0.04 | 0.36 ± 0.02 | 0.14 ± 0.04 | 0.36 ± 0.02 | 0.32 ± 0.04 | 0.23 ± 0.06 | 0.31 ± 0.5 | 0.22 ± 0.05 |
| 8 | 0.13 ± 0.04 | 0.35 ± 0.02 | 0.13 ± 0.03 | 0.36 ± 0.02 | 0.31 ± 0.03 | 0.20 ± 0.03 | 0.31 ± 0.04 | 0.20 ± 0.04 |

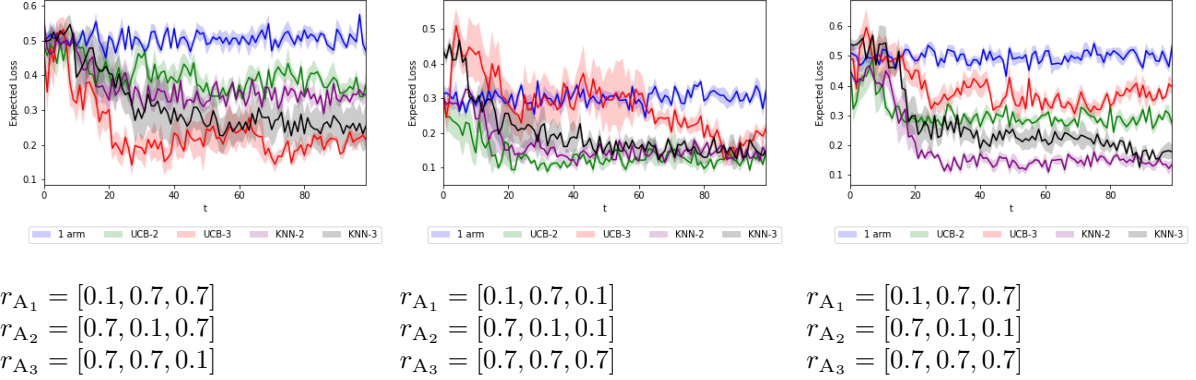


Figure 9: Loss plots over time for human simulations (denoted by r_{A_i}) in the CIFAR-3A setting.

do in our human subject experiments in Section 7. We indicate the simulated human competencies in the caption. We show how performance on a random sample of 100 points from a held-out set varies with time while learning a decision support policy. In general, we find that the more forms of support to learn, the longer it may take for the online algorithms to “converge.” For various simulations, KNN is more consistent in learning a decision support policy efficiently.

On the left, we find that LinUCB is good when each of the three arms are good at separate subsets of the data. KNN also performs well on such a task. In the middle, LinUCB is okay when we add a random arm and there is some overlap in the competencies of the arms. However, on the third pane, LinUCB is bad when we add a random arm and there is no overlap in competency; KNN handles fine (over time). We think this has to do with LinUCB’s inability to “turn off” any of the arms, i.e., there is no line configuration in input space that would lead to equiprobable selection of all arms.

D Additional User Study Details

D.1 Additional Recruitment Details

Within a task, participants are randomly assigned to an algorithm variant; an equal number of participants are included per variant (i.e., 10 for MMLU and 5 for CIFAR)⁷. Participants are required to reside in the United States and speak English as a first-language. Participants are paid at a base rate of \$9/hr, and are told they may be paid an optional bonus up to \$10/hr based on the number of correct responses. We allot 25-30 minutes for the CIFAR task and 30-40 for MMLU, as each MMLU question takes more effort. We applied the bonus to all participants.

D.2 CIFAR Task Set-up

We consider a 5-class subset of CIFAR (Bird, Cat, Deer, Frog, and Horse), as discussed in Appendix C⁸. We instantiate two forms of support: 1) a simulated AI model which provides a prediction for the image class, and 2) a consensus response derived from real humans, derived from the approximately 50 human annotators from CIFAR-10H [39, 100], presented as a distribution over the 5 classes.

We treat the original CIFAR-10 test set labels as the “true” labels and only include images for which the original CIFAR-10 label matches the label deemed most likely from the CIFAR-10H annotators (discrepancy was a rare occurrence, only 1.1% of the 5000 images considered). We sample a pool of 300 such images, and construct three different batches of 100 images. Participants are assigned to one batch of 100 images. Images per batch are sampled in a class-balanced fashion (i.e., 20 images for each of the 5 categories). Images are shuffled for each participant. The same latent codes (z_t) used in the computational experiments are employed for the user studies.

D.2.1 Corruptions and Support Design

We want to study whether our algorithms can properly learn which forms of decision support are actually needed by real humans. We therefore need to ensure that the task is sufficiently rich such that humans do *need* support (and the exist forms of support which can be of value). To mimic such a setting in CIFAR, we deliberately corrupt images of all classes except one (i.e., Birds⁹) when presenting images to the user. Corruptions are formed via a composition of natural adversarial transformations proposed in Hendrycks et al. [36], specifically shot noise ontop of glass blur. This enables us to check that our algorithms are able to properly recommend support for all other classes, as a human will be unable to decide on image category unassisted. Example corrupted images can be seen in Figures 15, 16, and 17

To ensure that the available forms of support have different regions of strength, we enforce that each form of support is only good at two of the five classes. In the case of the simulated AI model, we return the “true” class whenever the image is a Deer or Cat classes, and return one of the incorrect classes for all other images. For the consensus labels, we use the CIFAR-10H distribution derived from 50 annotators when the image is a Horse or Frog. As the CIFAR-10H labels were originally collected over all 10 CIFAR classes, sometimes an annotation was endorsed for a class outside of the 5 we consider; in that case, we discard the annotations assigned to those classes and renormalize the remaining distribution (on average, $< 2\%$ of the original labeling mass was discarded per image). For all other classes, we intend the consensus to be an unhelpful form of support, as such, for images in the Bird, Deer, and Horse class, we return a uniform distribution (i.e., providing no information to the participant).

D.2.2 Algorithm Parameters

For KNN, we take $K = 8$, $W = 25$, and $\epsilon = 0.1$; for both algorithms, we let $\alpha = 1$. Cost of either model arm is 0.5. For each algorithm, we consider two different settings of λ ($\lambda \in \{0.75, 1.0\}$ and $\in \{0.85, 1.0\}$ for KNN and LinUCB respective), selected using the hyper-parameter selection methods per Section 4.2. Using the population-level data per Appendix D.4, we select the (1) most likely λ and (2) the most

⁷Due to a server-side glitch, 6 of the 125 recruited participants received incorrect feedback on $\leq 2\%$ of trials.

⁸We explored a 3 class variant for HSEs to directly match the computational experiments; however, we realized that participants were able to figure out that which classes were impoverished, raising the base rate of correctly categorizing such images. Such behavior again highlights the need to carefully consider real human behavior in adaptive decision support systems.

⁹We further disambiguate the non-corrupted bird class by upsampling to 160x160 images via Lanczos-upsampling following [39, 100, 81] before presenting them to participants.

conservative λ . Since (1) and (2) led to the same $\lambda = 1$ for LinUCB with the collected population, we use the most likely λ with lowest cost.

D.3 MMLU Task Set-up

Participants respond to 60 multiple choice questions, which were balanced by topic (15 questions per topic). Participants are assigned to one of three possible batches of 60 such questions. Order is shuffled. Participants are informed of the topic associated with each question (e.g., that the question was about biology). We implement a 10 second delay between when the question is presented and when the participant is allowed to submit their response to encourage participants to try each problem in earnest.

D.3.1 Topic Selection

We ran several pilot studies with **Modiste** to determine people’s base performance on a subset of MMLU topics. We intended to select a set of diverse set of topics such that it was unlikely any one participant would excel at all topics – as many of the topics were specialized and at challenging [36] – but also varied enough that participants may be strong in at least one area. We found that a large number of participants achieved reasonable performance on elementary mathematics, and that a sufficient number of participants also excelled at questions in the high school biology, US foreign policy, and high school computer science topics – though usually not all together.

We also factored in **InstructGPT-3.5**’s performance while deciding on the topics. To best check whether our adaptive decision support algorithms are effective at learning good policies – like with CIFAR – it is helpful to have support available that is effective, should someone be unable to answer adequately alone. As a result, we looked more sympathetically on categories where model accuracy was already high.

However, the real-world is not so perfect: there may not be high-performing support available when a human struggles to make a decision. As such, we also deliberately forced down the accuracy of the LLM arm in the mathematics topic. While we expect that most participants would be able to solve elementary mathematics problems without the aid of the LLM support, should they be unable to, the LLM was not able to help them. We leave further impoverishing studies which mimic real-world support settings for future work.

D.3.2 Question Selection and Model Accuracy

The resulting accuracy of the LLM arm on the questions shown to humans per topic is: 29% for elementary mathematics, 89% for high school biology, 87% for US foreign policy, and 91% for high school computer science. We upweighted selection of foreign policy questions that participants in our pilot had gotten correct when constructing the question subset, as we wanted to ensure that, should a participant have foreign policy experience, they would be able to answer them.

D.3.3 Algorithm Parameters

We use the same parameters as in the CIFAR task, with the exception that we set the cost of support (i.e., the LLM arm) to 0.1. Additionally, we employ different λ – $\lambda \in \{0.6, 0.75, 0.9\}$ for KNN and $\lambda \in \{0.95, 1.0\}$ for LinUCB – selected using the hyper-parameter selection methods per Section 4.2. Using the population-level data per Appendix D.4, we select the (1) most likely λ , (2) most likely λ with lowest cost, and (3) the most conservative λ . Note that (1) and (2) yield the same λ for LinUCB.

D.3.4 Participant Comments Hint at Mental Models of AI

We observed that several participants in our MMLU task noted¹⁰ that their responses were biased by the AI. We include a sampling of comments provided by participants which we found particularly revealing. We believe that these responses motivate the need for further study of how users’ mental models of AI systems inform their decision-making performance, particularly in light of the rapidly advancing and public-facing foundation models [5].

- “I thought the AI answers went against my previous notions about what an AI would be proficient at answering. I thought an AI would excel at anything where there is a

¹⁰We included a post-experiment survey where we permitted participants to leave general comments.

set answer such as math, computer science coding question, and biology textbook definitions. Then I expected it to absoutly fail at political, and historical questions. Since they can be more opinionated and not have a definitive answer. However, the AI struggled with math and excelled in the other topics. So I was actively not choosing to agree with the AI on any math where I could also easily check its work and was heavily relying on it for everything else [...] I knew nothing about any question on computer science, so I mainly relied on AI for answers on that topic.”

- “AI seemed to me more helpful in topics I didn’t know, but sometime I trusted it too much, instead of thinking the answer through”
- “The AI had me second guessing myself sometimes so it affected my answers occasionally.”
- “Anything highlighted with the AI I was confident that would be the right answer.”

D.4 Constructing the Population Baseline

We recruit 20 participants from Prolific (via the same recruitment scheme as Section D.1) to estimate the population-level parameters (10 for MMLU and CIFAR, each). On each trial, participants are randomly assigned a form of support; trials are approximately balanced by arm type and grouping (i.e., topic or class). We compute participant accuracy averaged over all trials (100 for CIFAR, 60 for MMLU).

D.5 Visualizing Learned Policies

We provide additional details on how the policy generalization snapshots in Figure 5 are constructed. We save out the parameters learned by each algorithm while a participant interacts with **Modiste**. After the 60 or 100 trials (depending on which task they participated in), we load in the final state of parameters. We sample the embeddings of *unseen points* from the respective task dataset (as described in Appendix C) and pass these through the respective algorithm (LinUCB or KNN, depending on which variant the participant was assigned to) – yielding a recommended form of support for said embedding. We color the latent by the form of support. We draw randomly 250 such unseen examples for CIFAR, and 100 for MMLU, when computing the policy recommendations.

D.5.1 Additional Details of the Participants Included in Figure 5

The average loss and cost (averaged over the last 10 timesteps) for each of the participants depicted in Figure 5 are as follows: CIFAR ($r = 0.2$ and $c = 0.35$ for the participant sampled from those who saw the $\lambda = \text{KNN}$ variant, and $r = 0.4$ and $c = 0.15$ for the participant sampled from the $\lambda = \text{LinUCB}$ variant); MMLU ($r_I = 0.2$, $r_{II} = 0.2$, $r_{III} = 0.3$ and $c_I = 0.05$, $c_{II} = 0.05$, $c_{III} = 0.09$ for Participants I, II, and III respectively where the subscript indicates the associated participant). Participants I and II are drawn from the $\lambda = 1.0$ LinUCB variant, and Participant III is drawn from the KNN ($\lambda = 0.75$) variant. Participants’ learned policies depicted for CIFAR are randomly sampled. For MMLU, we select examples based on participants’ topic accuracies to highlight individual differences. Participant accuracies, when not receiving LLM support, are as follows: Participant I = [81.2%, 100%, 0.86%, 0.8%], Participant II = [80%, 0%, 0%, 50%], and Participant III = [43%, 25%, 25%, 75%], ordered as [math, biology, CS, foreign policy]. When interpreting accuracies, it is worth noting that as the algorithms are adaptive, the number of examples participants saw per topic varied. We include snapshots for participants, across both tasks, in Figures 10 and 11. We depict all CIFAR examples and a random sampling of 7 of the 10 participants per variant for MMLU.

D.6 Additional Reliance Investigations

While we find a likely relationship between a participants’ sensibilities of reliance and the incurred loss of the learned policy (see Section 7), we observe no strong relationship between reliance and incurred cost.

D.7 Interface

We include screenshots for the CIFAR (Figures 14 15, 16, and 17) task. Here, we highlight the differences in image quality presented to participants during the task; images are drawn from the *same* dataset (i.e., CIFAR-10 [35]), but in Figure 15, the image is *corrupted* (see Section D.2). We include screenshots from the MMLU task in Figures 18 and 19.

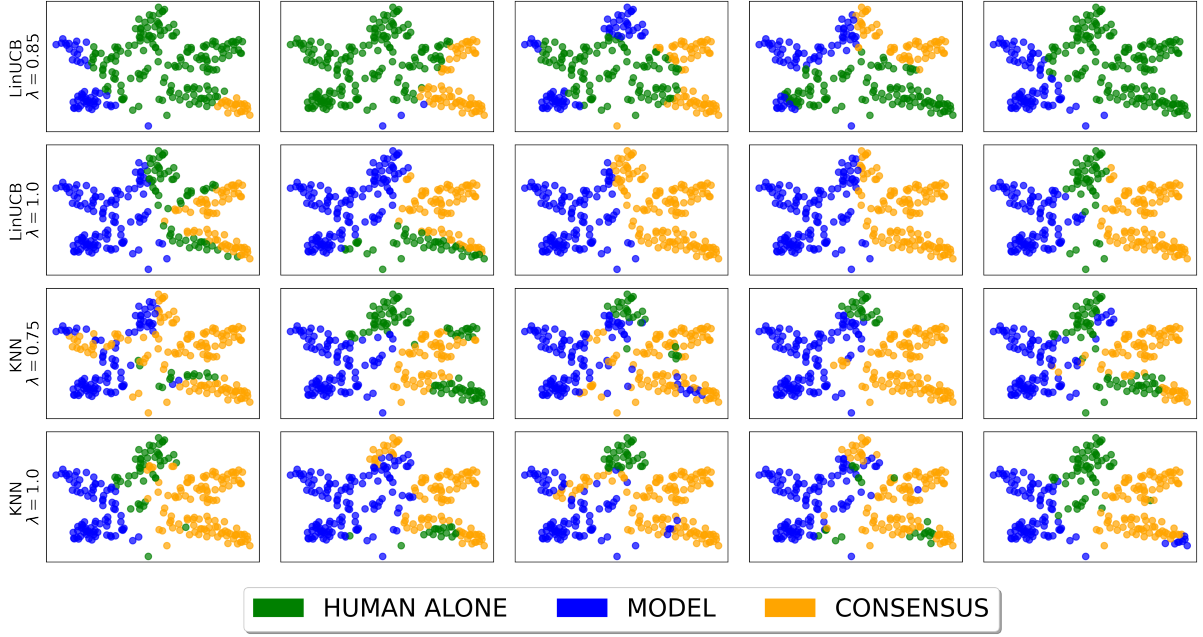


Figure 10: Snapshots of the recommended forms of support learned via *Modiste* for all participants in the CIFAR task, for different λ . Policies learned using KNN get closer to optimal; see Figure 5.

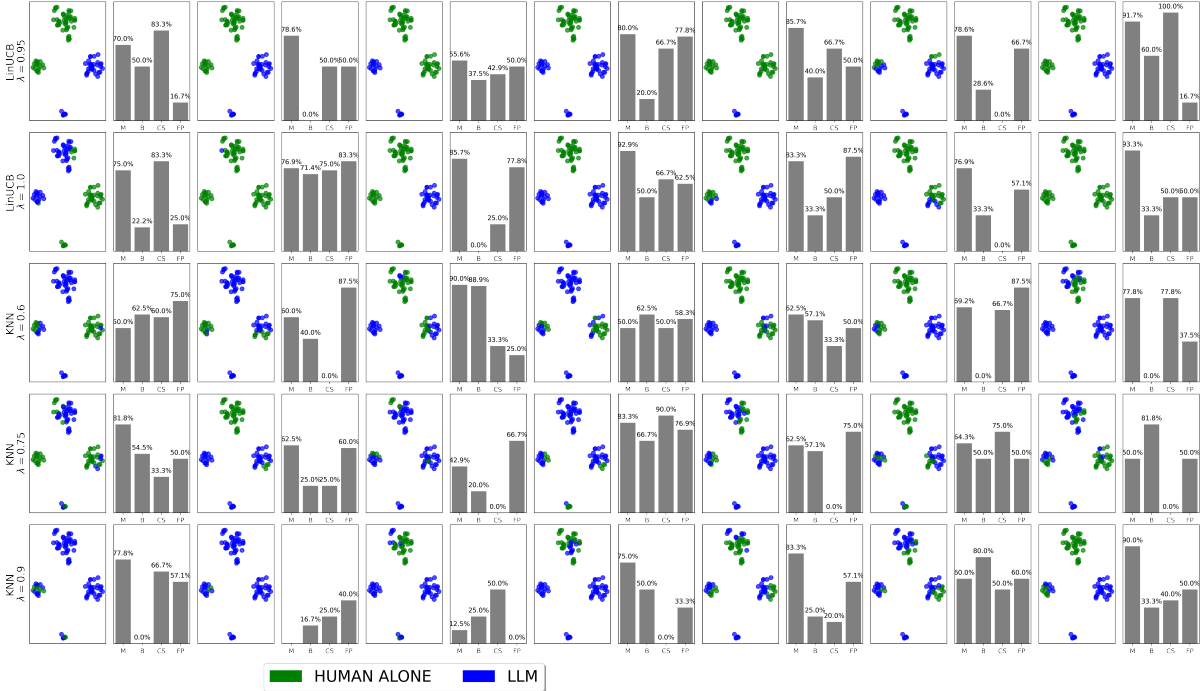


Figure 11: Highlighting individual differences in recommended support policies learned via *Modiste* for participants in the MMLU task. Topics are labeled as in Figure 5; clockwise from the top: math (M), biology (B), computer science (CS), foreign policy (FP). Adjacent to each policy visualization, we depict each participants' *unassisted* accuracy per topic; i.e., the accuracy for DEFER arms. We sample 5 participants out of the 10 per variant.

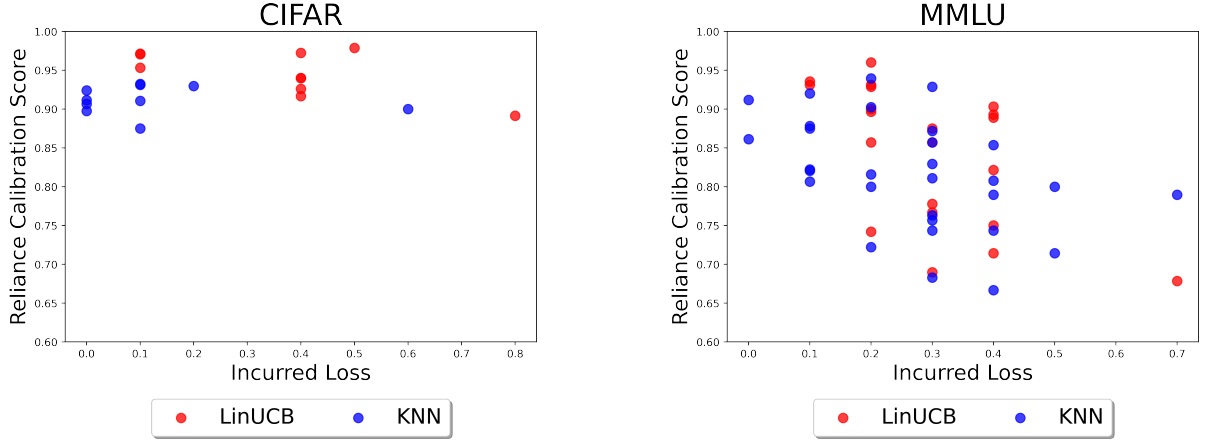


Figure 12: Relationship between a participants’ sensibility of reliance (measured as the proportion of times they correctly agreed or disagreed with the form of support’s prediction) and the loss incurred by the learned policy for the participant. Reliance is computed over all trials (100 for CIFAR, 60 for MMLU), and loss is averaged over the final 10 timesteps. We uncover an inverse relationship between reliance sensibility and the performance of learned policies for MMLU.

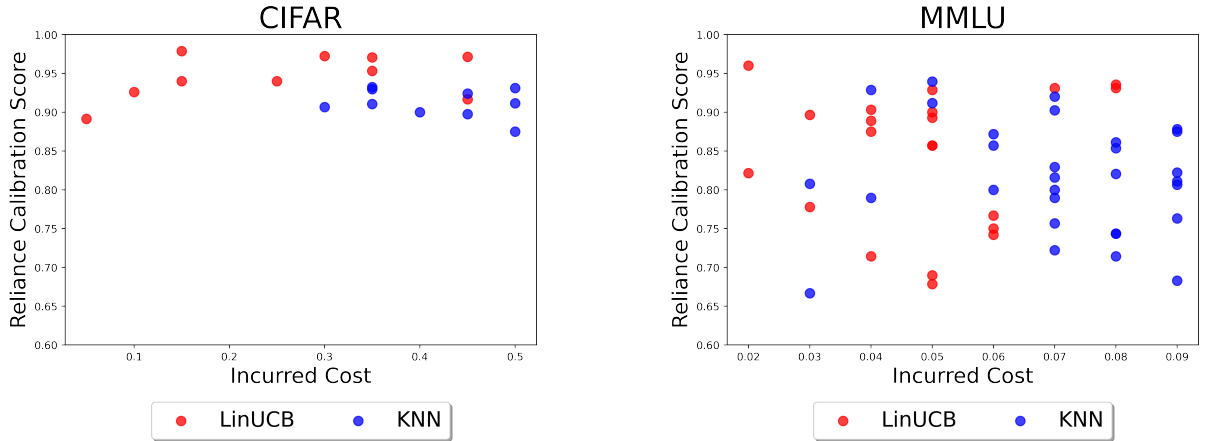
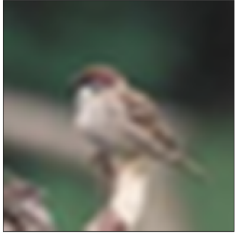


Figure 13: There is not a strong relationship between a participants’ sensibility of reliance (measured as the proportion of times they correctly agreed or disagreed with the form of support’s prediction) and the cost incurred by the learned policy for the participant.

What is Depicted in This Image?

Please decide which category is shown in the image below.



YOUR ANSWER

Please select a category

Bird ▼

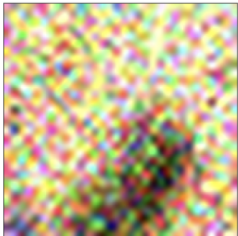
SUBMIT

Your Score:
3 out of 10 correct
30%

Figure 14: Example CIFAR interface for the HUMAN ONLY arm.

What is Depicted in This Image?

Please decide which category is shown in the image below.



AI Model Prediction

- Horse -

YOUR ANSWER

Please select a category

Bird ▼

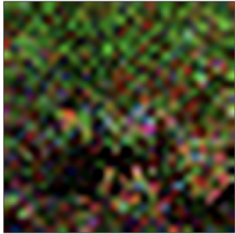
SUBMIT

Your Score:
15 out of 27 correct
56%

Figure 15: Example CIFAR interface for a MODEL arm.

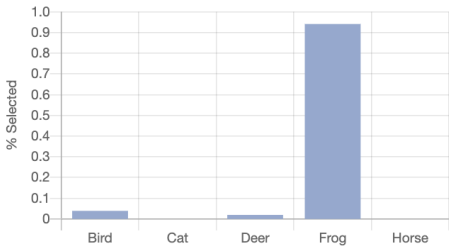
What is Depicted in This Image?

Please decide which category is shown in the image below.



Your Score:
9 out of 17 correct
53%

EXPERTS' OPINIONS



| Category | % Selected |
|----------|------------|
| Bird | 0.05 |
| Cat | 0.00 |
| Deer | 0.02 |
| Frog | 0.95 |
| Horse | 0.00 |

YOUR ANSWER

Please select a category

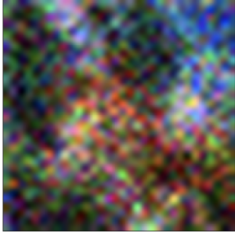
Frog ▼

SUBMIT

Figure 16: Example CIFAR interface for a CONSENSUS arm, using CIFAR-10H labels.

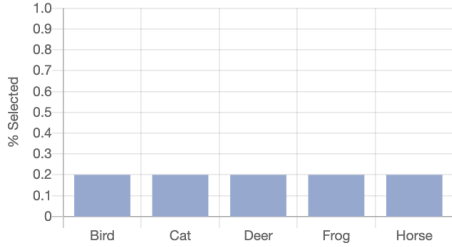
What is Depicted in This Image?

Please decide which category is shown in the image below.



Your Score:
10 out of 18 correct
56%

EXPERTS' OPINIONS



| Category | % Selected |
|----------|------------|
| Bird | 0.2 |
| Cat | 0.2 |
| Deer | 0.2 |
| Frog | 0.2 |
| Horse | 0.2 |

YOUR ANSWER

Please select a category

Bird ▼

SUBMIT

Figure 17: Example CIFAR interface for a **CONSENSUS** arm when the form of support is intended to be unhelpful.

Please answer the question about **mathematics** by selecting exactly one of the answers below.

Your Score:
2 out of 2

Which equation represents 36 less than a number, y , is equal to 13?

☐ $y - 36 = 13$
☐ $36 - y = 13$
☐ $13 - y = 36$
☐ $36 + y = -13$

SUBMIT

Figure 18: Example MMLU interface for the **HUMAN ONLY** arm.

Please answer the question about **biology** by selecting exactly one of the answers below. If an answer is marked in yellow, it is the prediction of an AI model.

Your Score:
3 out of 3

Lampreys attach to the skin of lake trout and absorb nutrients from its body. This relationship is an example of

- ☐ commensalism
- ☒ parasitism
- ☐ mutualism
- ☐ gravitropism

SUBMIT

Figure 19: Example MMLU interface for the LLM arm.